Soil Dynamics and Earthquake Engineering

A GIS procedure for the topographic classification of Italy, according to the seismic code provisions

--Manuscript Draft--

Manuscript Number:	SOILDYN-D-21-00049R2
Article Type:	Research Paper
Keywords:	DEM; Topographic classification; EC8; NTC18; GIS; Morphometric analyses
Corresponding Author:	Claudia Mascandola INGV: Istituto Nazionale di Geofisica e Vulcanologia ITALY
First Author:	Claudia Mascandola
Order of Authors:	Claudia Mascandola
	Lucia Luzi
	Chiara Felicetta
	Francesca Pacor
Abstract:	In this study we present a procedure for the topographic classification of Italy, taking advantage of existing high-resolution digital elevation models (DEM), with the support of routines embedded in Geographic Information Systems. The proposed method is based on morphometric analyses of a DEM, allowing for hilltop ridge detection, slope computation, identification of reliefs with potential topographic site effects, and topographic classification according to the indications of the current European and Italian seismic codes. The developed procedure can be applied worldwide and has a potential engineering interest for a fast and accurate topographic classification of a site, for both scientific and application purposes. The topographic classification of Italy is tested on several well-known cases of topographic amplification and it is adopted for the topographic classification of Italian accelerometric stations.
Suggested Reviewers:	Emilia Fiorini Eucentre emilia.fiorini@eucentre.it Expert in GIS and site effects
	Iunio Iervolino Universita degli Studi di Napoli Federico II Facolta di Ingegneria: Universita degli Studi di Napoli Federico II iunio.iervolino@unina.it Expert in Earthquake Engineering
	David Wald USGS: US Geological Survey wald@usgs.gov Expert in site effects and topographic data
	Nikolaos Theodoulidis ITSAK ntheo@itsak.gr Expert in site effects
	Maria Rosa Gallipoli IMAA-CNR: Istituto di Metodologie per l'Analisi Ambientale Consiglio Nazionale delle Ricerche mariarosaria.gallipoli@imaa.cnr.it Expert in site effects
Response to Reviewers:	

Response to Reviewer #2:

1. The answer to my first two concerns is not fully satisfactory since the main point is missed. I try here a new formulation of this point. The amplification coefficients reported in the seismic code is the result of numerical simulations relative to a limited set of morphological profiles. When one considers other configurations (e.g., the 'unclassified' ones in Pessina and Fiorini, 2014) applicability of the same coefficients is not warranted. Thus, the reduction of 'unclassified' sites is not necessarily a positive evidence encouraging the application of the new approach: actually, it may represent an unproper application of the procedure outside its actual domain. Other terms, the question is: at what extent the amplification coefficients can be actually applied to the configurations you have identified and were missed by Pessina and Fiorini? This is the point, which, in my view, should be addressed. Of course, I not asking for a revision of the procedure the Authors propose, but only a clear statement (to be reported in the 'Conclusion' section also), about this key aspect.

Pessina and Fiorini missed some configurations, since they did not use at the same time the concept of slope and ridge. In their tables 3 and 4, they make use of qualitative terms, like "close" and the classification of the site is driven by a rather subjective approach. This is why some of the configurations are missed. In our case, we make use of a quantitative approach, so that we can specify, for each pixel, the difference in height, the slope, the presence of a ridge, through the use of filter operators with specific dimensions that allow us to evaluate both ridge and slope, contemporarily. An example for the limit of the Pessina and Fiorini procedure is visible in their table 3, in case of the combination of R0-S3 codes (where sites are Not directly classified). The authors state that "stations are generally classified as T2, it is impossible to detect if they are at the base of slope, in the middle of slope, near terraces or in narrow valley".

2. I am not sure that when hazard (S1, S2, etc.) is evaluated at the same sites where maximum intensity were assessed, no "significant differences" are observed. A comparison between Figs. 2a and 2b in the answer puts in evidence important differences in the distribution of sites in the morphological classes T4 (and T2) relative to S3 and S4 hazard classes. When Figure 2b is compared with figure 7c, the respective patterns appear quite similar. Thus, the statistical significance of eventual differences (possibly induced by topographical amplification effects) should be assessed in some quantitative way. This is an important aspect to convince skeptical colleagues (including myself) that topographical features (at least the ones identified by the Authors) generally play a significant role in seismic hazard.

To address this point, we have reformulated the paragraph 'Statistics on the topographic classification map'. In particular, we have added a new figure (current Figure 7) with statistics on the 15332 Italian localities in DBMI15, grouped on the base of maximum observed macroseismic intensity at a site (Imax).

As described in the manuscript, in our opinion Figure 7 shows two aspects.

1. *A relation between Imax and the seismic zones (S1-S4).*

   "The localities with the lowest Imax (Figure 7a) are, of course, occurring in correspondence of the lowest seismic hazard zones (S3 and S4, ag ≤ 0.15) in Northern Italy, whereas the highest intensities are observed in correspondence of seismic hazard zones S1 and S2 (ag > 0.15) in the Central-Southern Apennines (Figure 7d). "

2. *A relation between Imax and the topographic classes (T1-T4).*

   "Based on the classification proposed in this study, about 40% of the localities with the Imax >6 could be affected by topographic amplification (T2-T4 classes, Figure 7c-d), in contrast to about 20% for Imax <6 (Figure 7a-b). Moreover, we observe a large occurrence of the sites with potential topographic amplification (T2-T4 classes) in correspondence of localities characterized by medium to high Imax (range 6 - 8), in seismic zone 2 (S2: $0.15 < ag \leq 0.25$), as shown in Figure 7c".

In conclusion: *based on our classification, the sites with potential topographic effects are clustered in zones with high seismic hazard (S1-S2 zones), where the higher macroseismic intensities are observed (Imax > 6).*
These results do not prove the existence of topographic amplification at those sites classified in T2-T4, but the coherency between the topographic classification (T1-T4), the maximum observed microseismic intensity (Imax) and the seismic hazard map, could be a hint of the occurrence of topographic effects. The concern of the reviewer about the significant role of topographic effects in seismic hazard will be further investigated in a future study that takes into account the residual distributions computed from Intensity Prediction Equations (IPE).

- Topographic classification of Italy according to the Italian seismic code
- Novel GIS procedure
- Around one third of the Italian territory has sites with possible topographic amplification

A GIS procedure for the topographic classification of Italy, according to the seismic code provisions

Claudia Mascandola[a*], Lucia Luzi[a], Chiara Felicetta[a], Francesca Pacor[a]

[a] Istituto Nazionale di Geofisica e Vulcanologia, Sezione di Milano, Milano, Italy

[*] Corresponding author. E-mail address: claudia.mascandola@ingv.it

Abstract

In this study we present a procedure for the topographic classification of Italy, taking advantage of existing high-resolution digital elevation models (DEM), with the support of routines embedded in Geographic Information Systems. The proposed method is based on morphometric analyses of a DEM, allowing for hilltop ridge detection, slope computation, identification of reliefs with potential topographic site effects, and topographic classification according to the indications of the current European and Italian seismic codes. The developed procedure can be applied worldwide and has a potential engineering interest for a fast and accurate topographic classification of a site, for both scientific and application purposes. The topographic classification of Italy is tested on several well-known cases of topographic amplification and it is adopted for the topographic classification of Italian accelerometric stations.

Keywords: DEM, Topographic classification, EC8, NTC18, GIS, Morphometric analyses

Supplementary data. The topographic classification of Italy is available in the electronic supplement.

1. Introduction

One of the possible causes of damage during earthquakes is the seismic waves amplification due to topographic irregularities. The reasons for topographic amplification may be several: the resonance of the whole relief when the incident seismic field has a predominant wavelength comparable to the horizontal width of the

mountain [1]; the focusing of seismic waves near the crest because of the reflection on a free surface and/or the interaction between incident and diffracted waves [2]. Moreover, topographic seismic amplification is considered as one of the possible causes of triggers of earthquake induced phenomena, like landslides, which represent one of the major causes of earthquake-related devastation (e.g. Refs. [3,4]). Several studies over the last four decades have discussed the effects of surface topography on seismic ground motions from instrumental investigations [5-12] and numerical models [13, 14, 4, 15, 16]. Relevant macroseismic case histories are reported by several authors [17, 18, 4, 19, 20, 21]. The proper assessment of topographic amplification is of key importance in the European context, where a broad range of exposure levels to earthquake hazard is encompassed [18] and many small towns are located at the top of isolated steep cliffs. Such unfavourable conditions often come together with high vulnerability of the buildings and the susceptibility to slope sliding [4]. Therefore, the topographic amplification, even if generally do not exceed the stratigraphic one (e.g. Refs. [4, 22, 23, 24]), plays a significant role in seismic design, microzonation studies and hazard analyses.

The current Italian (NTC, 2018; hereinafter NTC18 [25]) and European (CEN, 2004; hereinafter EC8 [26]) seismic codes prescribe frequency-independent amplification factors not larger than 40%, based on the height and the slope of simple 2D relief configurations. The approach, introduced in the EC8, was further adopted by NTC (2008) [27] and the current NTC18, where four classes of topographic amplification are explicitly defined, as listed in Table 1. These categories refer to bidimensional configurations, such as elongated crests and ridges, and must be considered only when their height is greater than 30m.

Table 1: Topographic amplification factors prescribed by Italian seismic code (NTC18).

Topographic Class	Description	Amplification factor
T1	Flat surface, isolated slopes and cliffs with average slope angle $i \leq 15°$	1
T2	Slopes with average slope angle $i > 15°$	1.2
T3	Relief with ridge width much smaller than the base and average slope angle $15° < i \leq 30°$	1.2
T4	Relief with ridge width much smaller than the base and average slope angle $i > 30°$	1.4

Following the classification of the Italian seismic code, Ref. [24] first implemented a procedure for the topographic characterization of seismic recording stations archived in ITACA 2.0 database (Italian Accelerometric Archive, http://itaca20.mi.ingv.it/ItacaNet_20/; [28, 29]). The procedure is based on morphometric analyses of high-resolution digital elevation models (DEMs), with the support of Geographic Information Systems (GIS). In the specific, the procedure computes the slope and ridge layers from DEM, besides different statistical indicators (i.e., maximum, minimum, sum, and mean) within a circular buffer area around each recording station. These statistical indicators are combined to provide both a slope and a ridge index that are further matched to define the topographic classification of the seismic station. However, some combinations of the indices do not permit a univocal topographic classification because their arrangement may lead to different topographic classes (in that case the site is not classified). Moreover, the procedure implemented for the ridge detection is not straightforward and implies several noise removal steps to enhance significant features and remove small topographic irregularities. Since the procedure is applied to the surroundings of each seismic station, it needs to be run each time a new seismic station is added to the database. These downsides led to the development of a new GIS-based procedure for topographic classification of the whole Italian territory. However, the NTC18 prescribes the applicability of the topographic coefficients in case of "simple" configurations, but the criteria to discriminate between "simple" and "complex" are not specified and, for this reason, the applicability of the coefficients could be debated.

In this study, we propose a step-like procedure and provide some statistics of the resulting map, correlating it to the probabilistic seismic hazard [30, 31], the macroseismic intensity data in DBMI15 [32], and the seismic stations in the Italian Accelerometric Archive 3.1 (ITACA 3.1; http://itaca.mi.ingv.it/ItacaNet_31/#/home; [33]). The topographic classification is tested at several sites, where topographic amplification has been observed. Finally, based on the proposed classification, we evaluate the impact of the topographic amplification factors (Table 1), on the probabilistic seismic hazard map calculated for Peak Ground Acceleration (PGA), a return period of 475 years, and stiff soil i.e. soil class EC8-A [30].

2. Method

Digital elevation models (DEMs) are fundamental in environmental and morphological analyses. In this study, the topographic classification is applied to the so called *TinItaly DEM* [34], created for the whole Italian territory as a triangular irregular network (TIN), and converted into grid format of 10m cell size, according to a tiled structure composed of 193, 50-km side square elements. Ref. [34] carried out a comprehensive assessment of the accuracy of the TinItaly DEM, finding a root mean square error in elevation (RMSEz) between 0.8 and 6.0 m. For our analysis, we select the TinItaly DEM since, to date, it is the model with the highest resolution, freely available for scientific purposes for the whole Italian territory.

The morphological analyses applied on the DEM are summarized in Figure 1 and described in detail in the following subparagraphs. Starting from DEM (Figure 1, step 1), the slope angle is computed (step 2) along with the Topographic Position Index (TPI; [35], step 3) and the elevation range (maximum minus minimum elevation value in a moving window), applying a threshold height of 30 m (H30) and 60 m (H60), respectively (step 4). Since the positive TPI values allow detecting the ridge zones, an empirical threshold of 5 m is adopted to discriminate between ridges (ridge is assigned 1) and non-ridges (ridge is assigned 0). Considering the slope and TPI values, a first discrimination of topographic classes can be performed (Figure 1). Whereas T1 and T2 sites are on slopes (ridge = 0), T3 and T4 sites should be on ridges (ridge = 1). Therefore, T1 and T2 categories can be identified by the combination of ridge = 0, and slope angle $< 15°$ or $\geq 15°$, respectively (step 6); T3 and T4 classes can be identified by ridge = 1 (Figure 1, step 5), on reliefs with difference in height > 30 m. To further discriminate between T3 and T4 classes, the H60 map is considered. When H60 = 1 (elevation range

101 *H* is between 30 and 60 m) the site is in class T3 (step 6). In the following, the step-like procedure applied to
102 the TinItaly DEM is described in detail, indicating the ESRI ArcGis (www.esri.com) tools adopted for the
103 morphological analyses.
104

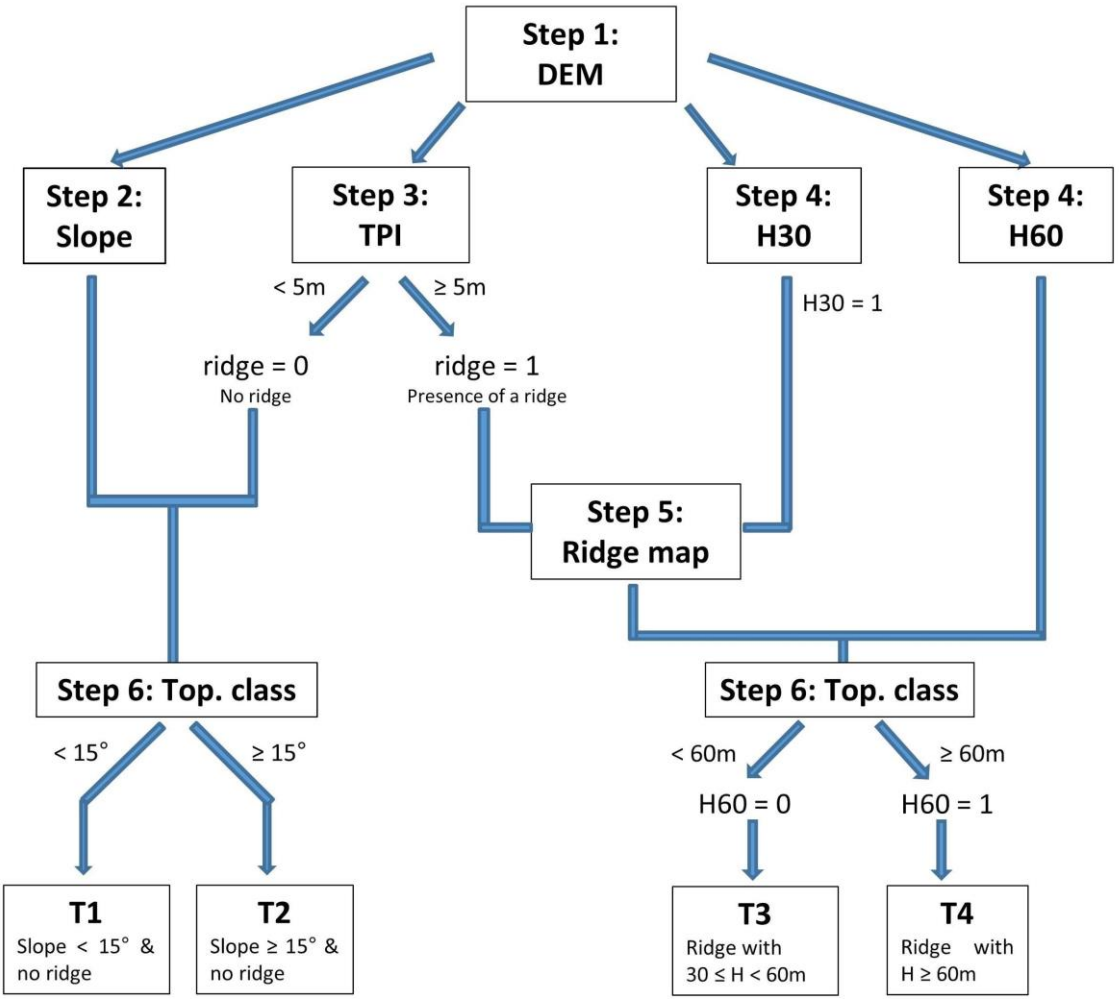

105

106 **Figure 1:** Workflow for topographic classification.

107

108 **Step 1: preliminary DEM processing**

109 To improve the computation time and data handling, the 193 TinItaly DEM tiles are resampled with a 40 m
110 resolution. Afterwards, the DEM tiles are merged to obtain a unique map for the Italian territory. Finally, to
111 remove minor irregularities, a smoothing is performed by applying a mean algorithm with a 3x3 moving
112 window (e.g. *Focal Statistics* tool in ESRI ArcGis), as shown in Figure 2a for a sample area in central
113 Apennines.

Step 2: computation of topographic slope

To compute the slope angle, we use the *Slope* function implemented on ESRI ArcGis (Figure 2b). The slope is computed in degree units in a 3 by 3 cell neighborhood (i.e., moving window) on the smoothed DEM, considering the planar method with the average maximum technique [36]. The slope is measured as the maximum rate of change in value from a cell to its immediate neighbors. The calculation is performed on a projected flat plane using a 2D Cartesian coordinate system. The processed cell is judged reliable if the computation is performed on at least seven cells in the 3 by 3 neighborhood.

Step 3: ridge extraction

For the ridge detection, we adopt the Topographic Position Index (TPI) algorithm proposed by Ref. [35]. This algorithm is implemented in the *Land Facet Analysis* toolbox [37] in ESRI ArcGis. The TPI is defined as a difference between the actual value of the elevation H at given location [x, y] and mean elevation of the neighboring area A:

$$TPI(x,y) = H(x,y) - \int_A H(x,y)\partial S \,/\, \int_A \partial S \qquad \text{Eq. (1)}$$

The area A should be centered at the point [x, y]. Both the size and the shape of the neighboring area have to be defined in advance, depending on the specific application. In general, there is no constraint on both values. The TPIs reflect the differences between the elevation in a particular cell and the mean elevation of the surrounding cells: positive values mean the cell is higher than its surroundings, while negative values mean it is lower. Therefore, high positive values of TPI characterize ridgetops and hilltops, while negative values define basins or valley bottoms. TPI values close to zero indicate flat or mid-slope areas. This kind of analysis strictly depends on the scale used to count the surrounding cells. To set the interval for the TPI analysis, we carry out some tests, considering different radii (i.e. 300 m, 500 m and 800 m). For the Italian case, a neighborhood circle with a radius of 500 m is adopted, since it allows better discriminating the ridges out of the main reliefs, while ignoring the minor deflections [38]. The ridge zones are obtained from the TPI map (*Raster Calculator* tool) considering a threshold value equal to 5. The output is a binary raster that takes the value 1 when TPI > 5 and 0 otherwise (Figure 2c). Since TPI units are in meters, a TPI value of 5 means that

this particular cell is 5 m higher than the average elevation of its neighborhood (i.e., a radius of 500 m). The TPI threshold is selected empirically. A lower threshold (down to 1) does not significantly affect the final results. The ridgelines are retrieved by applying a thinning function (*Thin* tool) that thins rasterized linear features by reducing the number of cells representing the width of the features [39], as shown in Figure 2d.

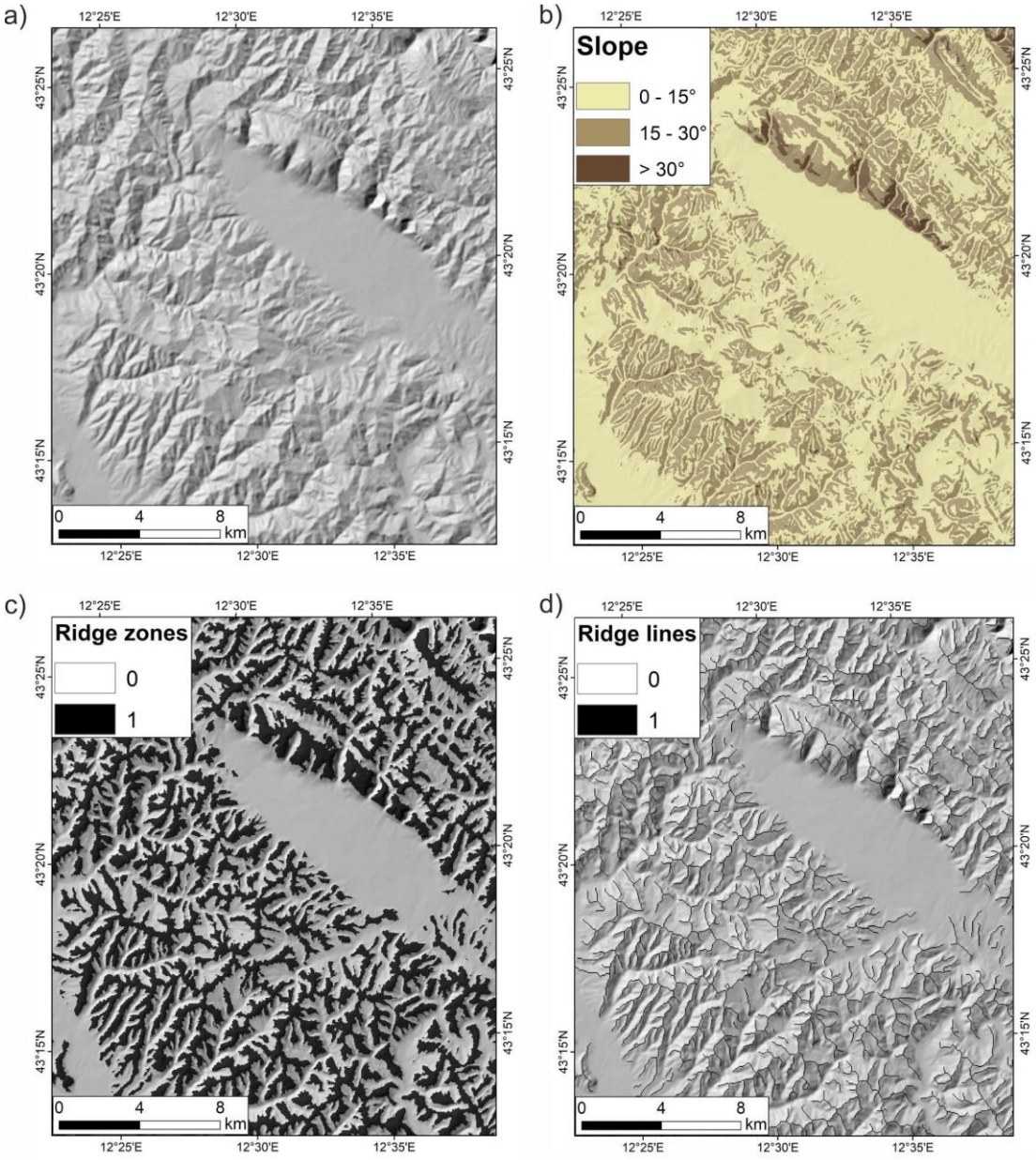

Figure 2: Extraction for an area of the Central Apennines of a) DEM, represented as hillshade; b) topographic slope; c) ridge zones setting TPI > 5; and d) ridge lines after thinning.

Step 4: detection of the difference in height to extract topographic categories T3 and T4

In the EC8 and NTC18 seismic codes, reliefs higher than 30 m are considered to have potential topographic site effects (i.e., T3 or T4 topographic classes in NTC18). To individuate these reliefs, we compute the

elevation range, i.e., maximum minus minimum elevation value, in 5x5 cells moving windows (Figure 3a; *Focal Statistics* tool). Considering that the DEM cell size is 40 m, the maximum and minimum semi-transverse axis of a relief spanned by a 5x5 moving window is 113 m (e.g. $80 \cdot \sqrt{2}$m), as exemplified by the dark grey line in Figure 3, and 40 m (light grey line in Figure 3), respectively. Considering a threshold difference in height of 30 m (condition for topographic amplification), we obtain the slope angle interval, which ranges between 14° and 37° (Figure 3b,c), thus including both T3 and T4 classes. To discriminate class T4, we consider the map representing the difference in height of 60 m that individuates the slope angles in the interval 27°-56° (Figure 3d,e), including T4 sites (i.e, ridges with height greater than 30 m and average slope angle $i >$ 30°). In the following sections, the elevation range computed with a threshold height of 30 m is indicated as H30; whereas the elevation range computed with a threshold height of 60 m is indicated as H60 (Figure 4).

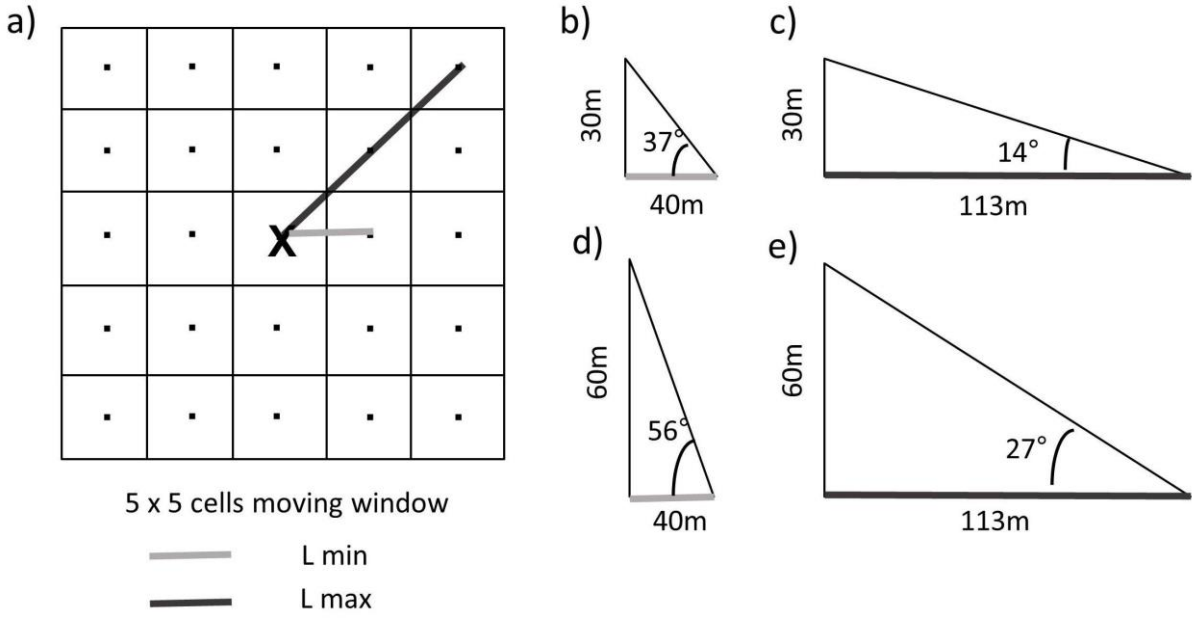

Figure 3: Trigonometry applied to H30 and H60 maps. a) 5x5 cells moving window with the smaller (light grey line) and larger (dark grey line) semi-transverse axis spanned in the moving window. b)-c) maximum and minimum slope angles, considering a difference in height of 30 m, d)-e) maximum and minimum slope angles considering a difference in height of 60 m.

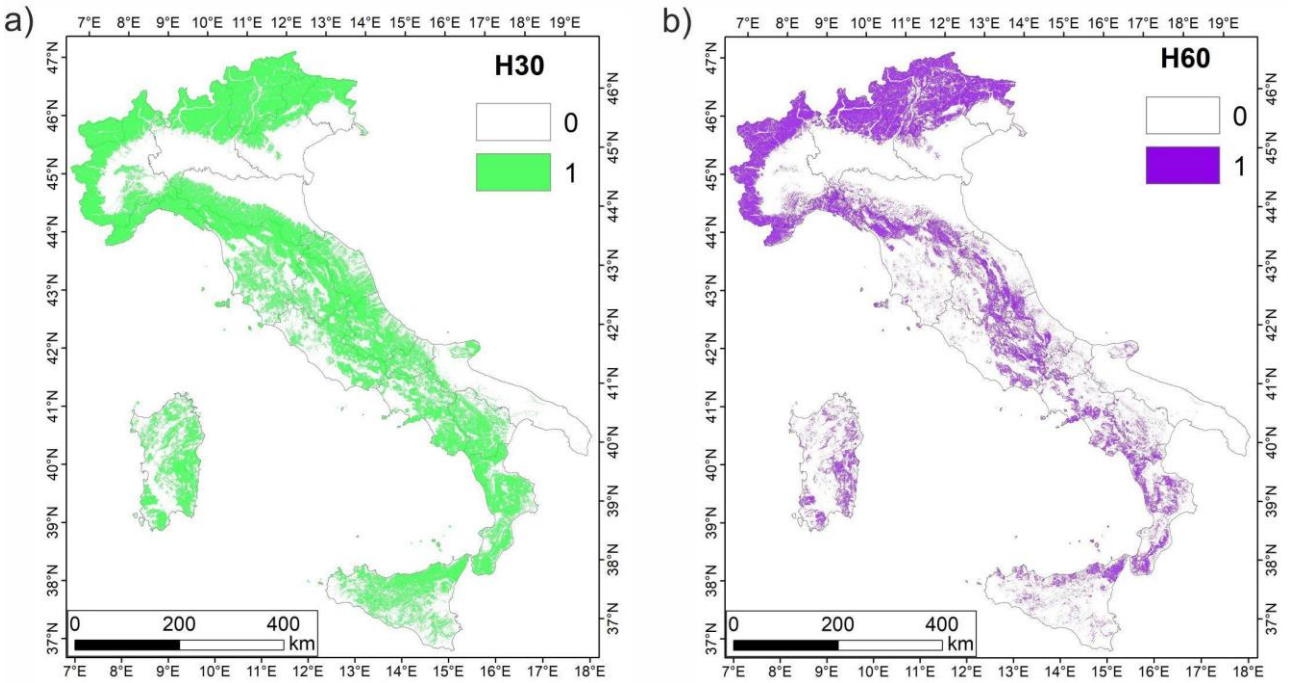

Figure 4: Map of a) difference in height of 30 m (H30) and b) 60 m (H60) for the Italian territory.

Step 5: identification of T3 and T4 topographic categories

After the identification of the difference in height to extract T3 and T4 topographic categories, the ridge lines of the corresponding reliefs can be obtained by overlapping the ridge line map (evaluated in step 3) and the H30 map (evaluated in step 4) (*Raster calculator* tool, imposing H30 =1 & ridge lines =1), as shown in Figure 5a. To identify the sparse groups of points (< 5 cells), the *Region Group* tool is combined with the *Set Null* operator. The *Region Group* counts the number of grouped cells within an 8-cells neighborhood (excluding 0 values), and the *Set Null* sets to null the cell values for counts less than 5. The sparse groups of points are finally removed with the *Nibble* operator that allows filtering of the ridge line raster. Finally, the extracted ridges are dilated (3 cells per side), using the *ArcScan* extension (Figure 5b). Being the raster cell size 40 m, the ridge lines are dilated by 120 m per side to approximate the semi-transverse axis of a relief with a minimum 30 m of difference in height and a consequent minimum slope angle of 15°, which are the thresholds for topographic amplification according to NTC18 and EC8 seismic codes (see Figure 3c as an example). In this sense, the 120 m per side is conservative because it may include the whole relief down to the base.

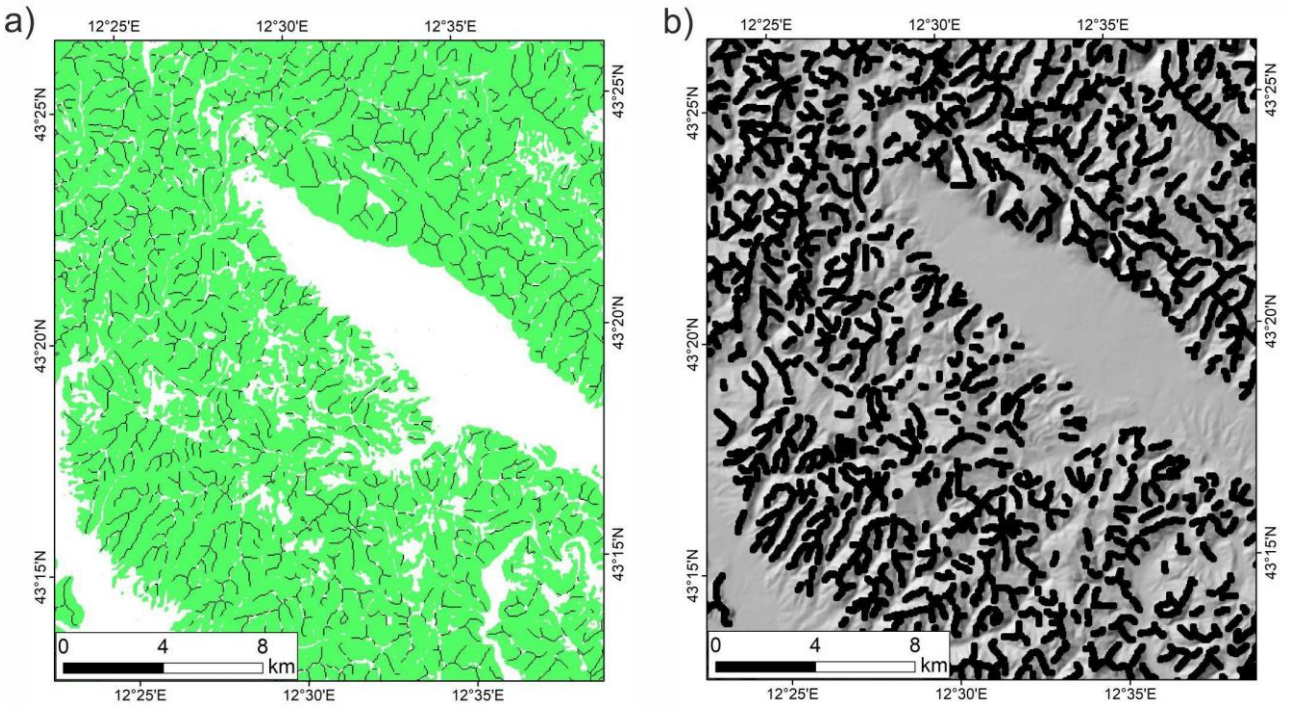

Figure 5: a) intersection between ridge line map (black lines) and H30 map; b) ridge map on DEM represented as hillshade.

Step 6: topographic classification

Once the identification of the morphological parameters is performed, the final topographic classification is obtained by combining the following maps:

1. slope angles (*slope* map);
2. ridges of reliefs with potential topographic amplification (*ridge* map);
3. reliefs with average slope angle $i > 30°$ (*H60* map);

as reported in Table 2 (*Raster calculator* tool). The final topographic classification is reported in Figure 6 and provided in the electronic supplement.

Table 2: Topographic classification (NTC18), based on the proposed GIS-procedure.

Condition	Class	Description
ridge = 0 & slope < 15°	T1	slope with average slope angle $i < 15°$
ridge = 0 & slope ≥ 15°	T2	slope with average slope angle $i \geq 15°$
ridge = 1 & H60 = 0	T3	ridge with difference in height in the range 30-60 m (i.e. base angle ≤ 30°)
ridge = 1 & H60 = 1	T4	ridge with difference in height > 60 m (i.e. base angle > 30°)

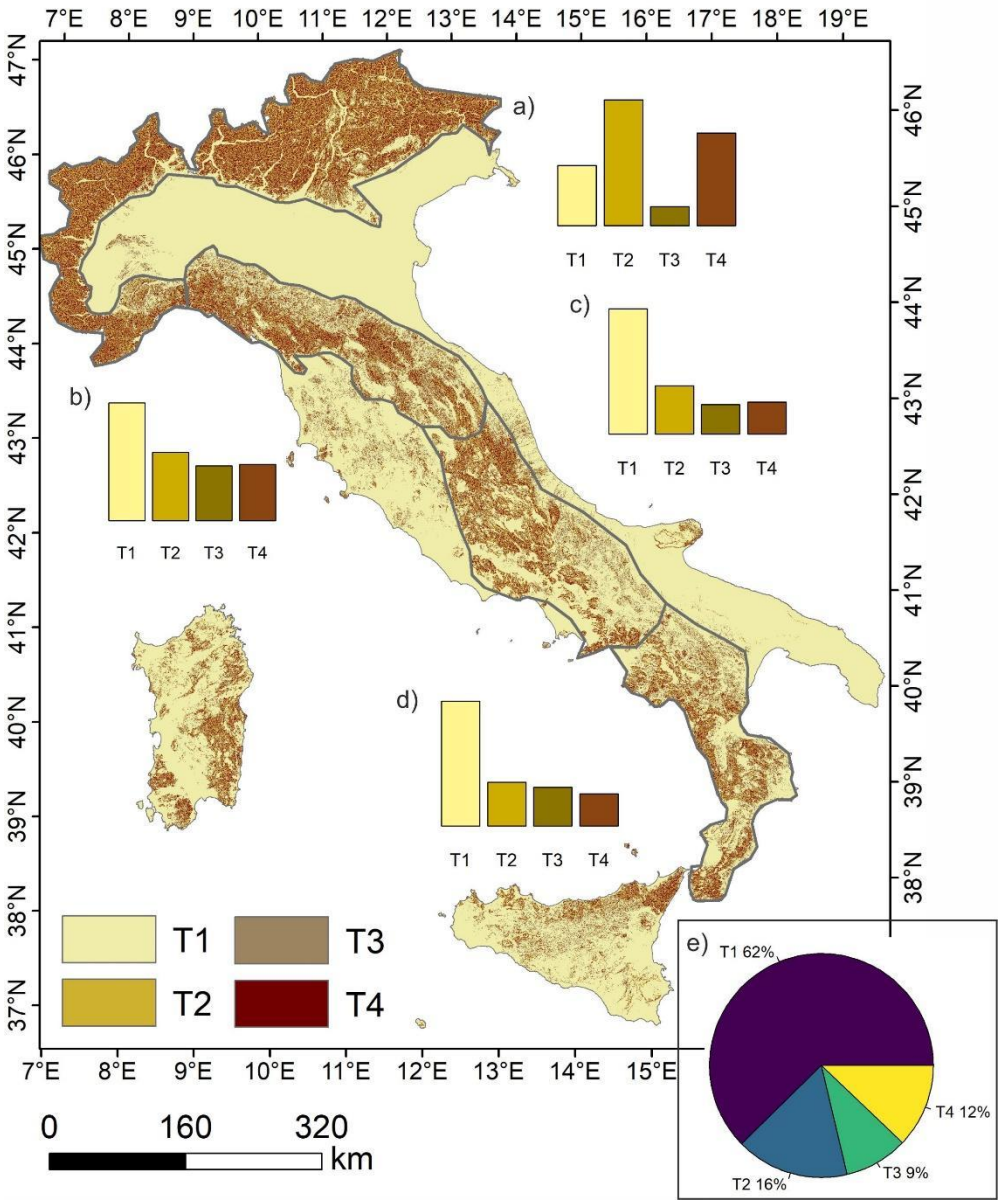

Figure 6: Topographic classification of Italy according to the current Italian seismic code (NTC18), obtained following the proposed procedure. The histograms of the topographic classes are reported for the Alps (a) and the Apennine (b, c, d) mountain chains, in the Northern, Central, and Southern sectors respectively (grey outline). e) Pie chart of topographic classes (T1-T4) for the whole Italian territory. The statistics are computed on a sample of 10,000 random points distributed homogeneously throughout the Italian territory. The count is normalized to the number of points in each sector.

3. Statistics on the topographic classification map

To provide an overview of the topographic classification map in Figure 6, some statistics are computed on a sample of 10,000 random points distributed homogeneously throughout the Italian territory, with a minimum interdistance of 50 m. Figure 6 shows the distribution of the topographic classes for different zones (i.e., Alps and Northern, Central, Southern Apennines). The Alps are characterized by prevalent T2 slopes (42%) and T4 ridges (31%) (Figure 6a), whereas the Apennines are characterized by prevalent T1 slopes (40-50%) with equally distributed T3 and T4 ridges (both are around 15-20%) (Figure 6b, c, d). Most of the Apennines reliefs are concentrated to the North (Figure 6b), where the percentage of T2, T3 and T4 classes is larger (~60%) than in the southern sector of the Apennines (~45%) (Figure 6 c,d). Overall, about one third of the Italian territory is characterized by sites with possible topographic amplification (i.e., T2, T3 and T4 classes in Figure 6e). In detail, 25% of Italian territory is characterized by sites in T2 or T3 (topographic amplification factor of 1.2, Table 1), whereas 12% of the country area is in T4 (topographic amplification factor of 1.4, Table 1) (Figure 6e).

In Figure 7, we show how the proposed topographic classes for the whole Italian territory are distributed with respect to the maximum observed macroseismic intensity (*Imax*, Mercalli-Cancani-Sieberg; [42]) at 15332 Italian localities in DBMI15 [32] and the seismic zones in Ref. [40] (S1-S4). As expected, the localities with the lower *Imax* (Figure 7a) are concentrated in the lower seismic hazard zones (S3 and S4, ag $\leq$ 0.15) of Northern Italy, moving gradually toward the higher seismic hazard zones (S1 and S2, ag > 0.15) of the Central-Southern Apennines for *Imax* > *8* (Figure 7d). When we also consider the topographic classification of this

study, about 40% of the localities with the higher *Imax* (>6) is affected by topographic amplification (T2-T4 classes, Figure 7c-d), in contrast to just about 20% for lower *Imax* (<6) (Figure 7a-b). Moreover, we observe a clusterization of the sites with possible topographic amplification (T2-T4 classes) in Figure 7c, with localities characterized by medium high *Imax* (between 6 and 8), localized in seismic zone 2 (S2: $0.15 < ag \leq 0.25$). These results do not prove the existence of topographic amplification at those sites classified in T2-T4, but the coherency between the topographic classification (T1-T4), the maximum observed microseismic intensity (*Imax)*, and the seismic hazard map, represented by the seismic zones S1-S4.

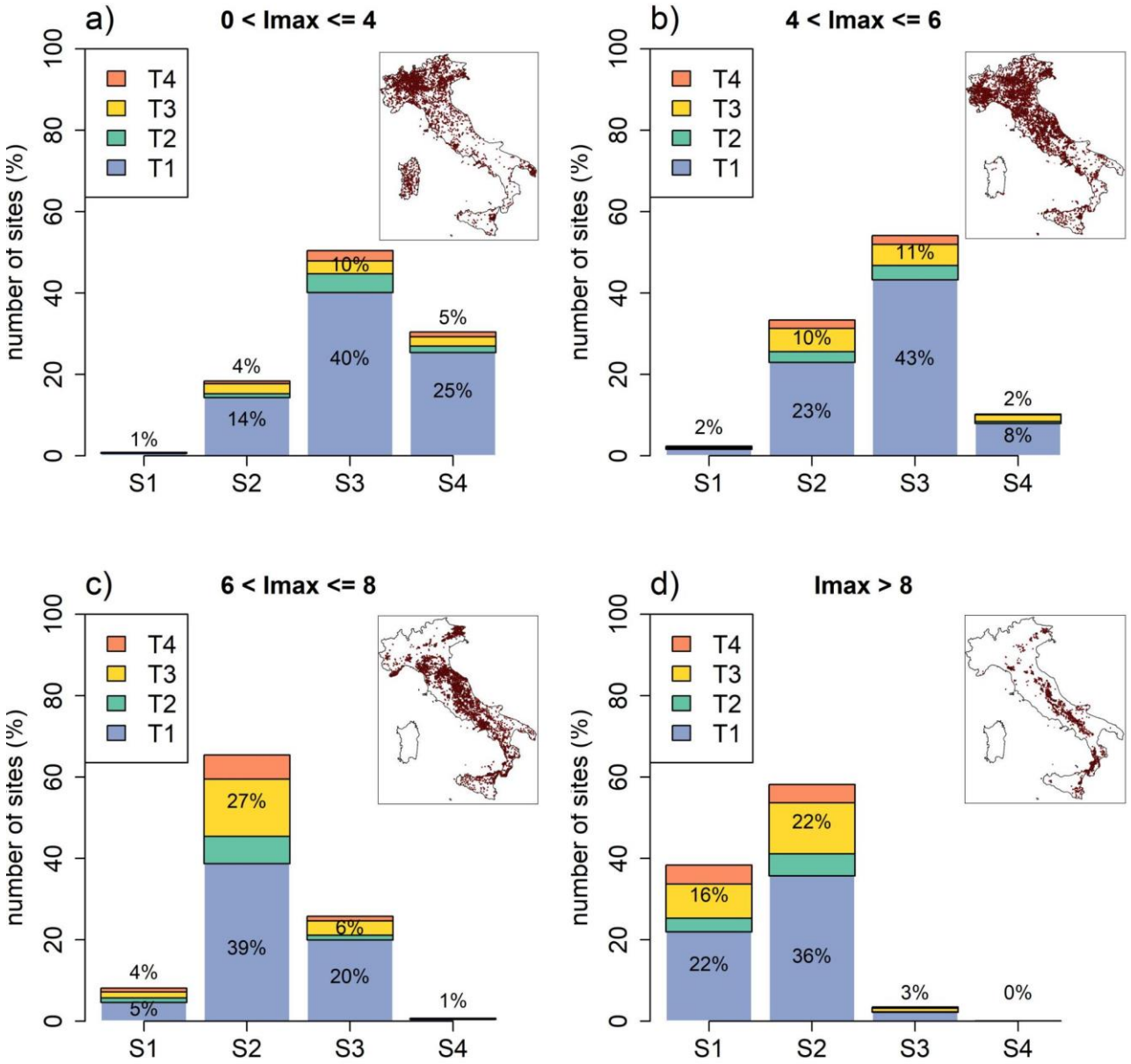

Figure 7: Statistics on the topographic classification of 15332 Italian localities in DBMI15 [32], grouped based on the maximum observed macroseismic intensity at a site (*I max*, Mercalli-Cancani-Sieberg; [42]). a) $I\ max \leq 4$, b) $4 < I\ max \leq 6$, c) $6 < I\ max \leq 8$, d) $I\ max > 8$. The percentages are normalized to the number of sites in each group. S1-S4 are the seismic zones in Ref. [40], and T1-T4 are the topographic classes in NTC18. The geographic distribution of each dataset in panels a)-d) is reported in the insets.

Finally, we classify the seismic stations archived in the ITACA 3.1 database according to the map in Figure 6. The stations of the Italian Strong Motion Network (RAN; http://ran.protezionecivile.it/IT/index.php) operated by the Department of Civil Protection (IT network code), and of the Italian National Seismic Network (RSN; http://cnt.rm.ingv.it/instruments/network/IV), run by National Institute of Geophysics and Volcanology (IV network code), are considered in Figure 8a and Figure 8b, respectively. The accelerometric sites, classified as T1, reflect the distribution in Figure 6e (62% of Italian territory is in T1); however the percentage of T1 sites in IV and IT networks is quite different (53% versus 68%, respectively, as in Figure 8). Indeed, most seismic stations of the IT network are installed in urban areas for civil protection purposes (Figure 8a), whereas many stations of the IV network are installed outside urban areas for seismic monitoring or scientific purposes (Figure 8b). Among the other topographic classes, both networks have a majority of T3 class for those stations on the Appennine ridges (Figure 8), whereas the T2 and T4 classes are distributed between the Alps and Apennine mountain chains (Figure 8). The percentage of T2 sites in the IT and IV networks is equivalent (~7%), but the percentage of T3 (17% for IT; 26% for IV) and T4 (6% for IT; 12% for IV) sites nearly duplicates moving from IT to IV network (Figure 8).

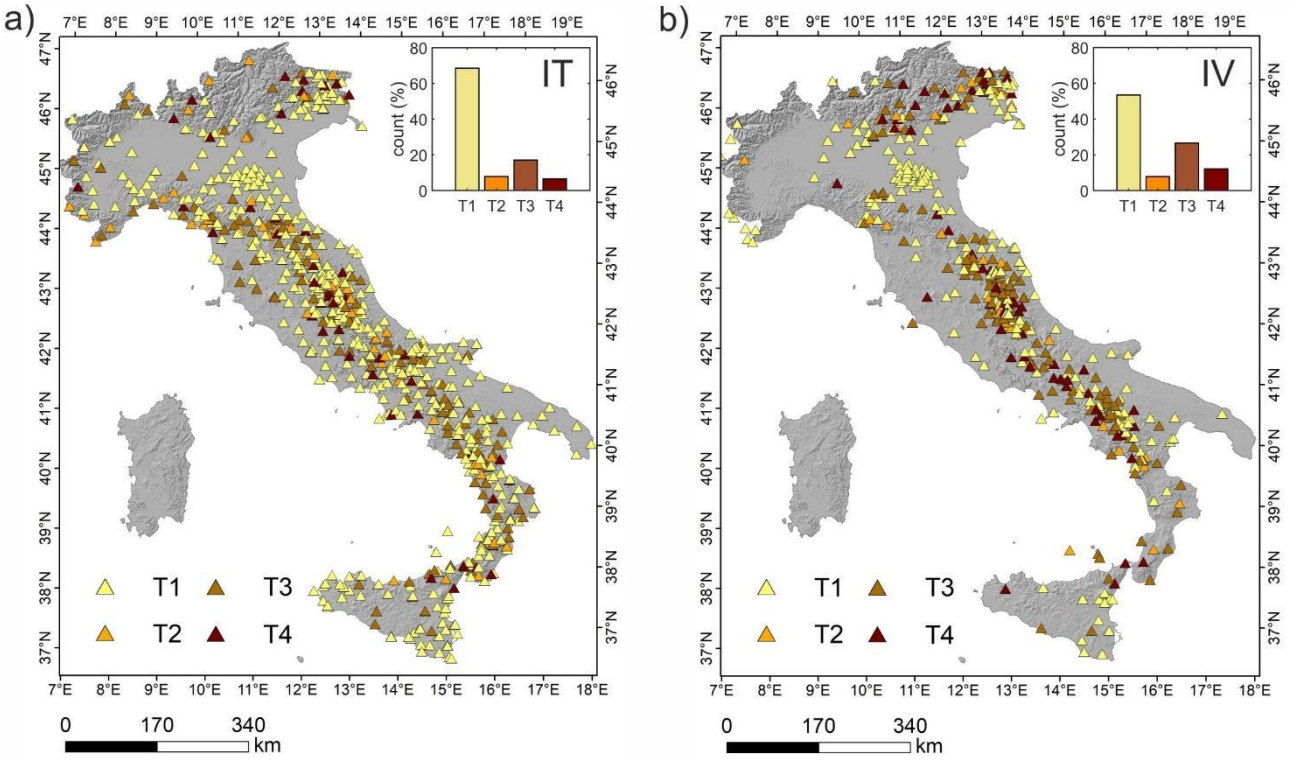

Figure 8: topographic classification for the seismic stations of the ITACA 3.1 database for the RAN network (a), and the RSN network (b). IT: network code of the RAN stations; IV: network code of the RSN stations.

4. Testing of the topographic classification on case studies

The proposed topographic classification is tested at different sites for which topographic amplification is well known (e.g. Refs. [43, 44, 10, 45, 46, 22, 23, 47]). In this study we consider Narni, Navelli, Nocera Umbra, and Assisi (Figure 9).

The seismic amplification of the Narni ridge was investigated through numerical modelling and empirical observations (e.g. Refs. [10, 46]), which proved the dependence of amplification on morphological features. The experimental evidence shows an amplification of the reference motion up to 2.2-3, for the spectral ordinates in the range 0.2-0.3 s (4-5 Hz). The largest amplifications are observed when the direction of the ground motion is perpendicular to the main axis of the ridge. Ref. [10] describe the Narni ridge as 220-m-high, with slopes ranging from 22° to 35°. According to the authors, the topographic class of the Narni ridge is T3

281 at the eastern end, and T4 at the western end, in agreement with the topographic classification of this study
282 (Figure 9a).

283 The Nocera Umbra hill was studied by several authors (e.g. Refs. [43-45]). The historical centre of Nocera
284 Umbra suffered MCS intensity VII–VIII, due to the M_W 5.7 and 6.0 Umbria–Marche earthquakes on 1997,
285 September 26th. The hill is elongated in the NNW–SSE direction, with a maximum height of 574 m a.s.l., and
286 a difference in height equal to 144 m. The northern side of the hill is quite gentle, while the southern one is
287 very steep, therefore the topographic profile along the major axis is asymmetric with a narrow ridge. In
288 contrast, the transverse section is more regular and symmetric, with a base width of about 400 m. Topographic
289 amplification effects are observed at about 3.5 Hz, where the polarization is transversal to the major axis of
290 the hill. The topographic classification map of this study (Figure 9b) reproduces the morphological features
291 described in Ref. [45], with a T3 class at the northern end of the relief, and a T4 class at the southern end.

292 The Navelli ridge was studied by Ref. [23]. The historical centre of Navelli is located along the south-western
293 slope of a NW-SE-trending narrow ridge, which is lithologically characterized by the outcropping crystalline
294 limestones. For this case study, a combination of topographic and stratigraphic amplifications was observed,
295 given a station on a rocky slope (in the historical center of Navelli) and one on a flat alluvial valley (at the base
296 of the hill). The mean slope angle along the historical center is 19° and considering that this morphological
297 ridge is much narrow at the top with respect to its base, the Navelli historical centre can be ascribed to the
298 topographic category T2 [23]. The topographic classification map of this study reproduces the morphological
299 features described in Ref. [23], but extends the ridge zone to the historical center of Navelli (Figure 9c) that,
300 for this reason, is classified in T3 instead of T2 class. In this regard, the topographic classification map is
301 conservative with respect to a more detailed observation at the site.

302 Finally, the ridge of Assisi, studied by Ref. [22], is presented. The station ASS
303 (http://itaca.mi.ingv.it/ItacaNet_31/#/station/IT/ASS) is located inside the Sacro Convento, near the historical
304 Basilica of San Francesco, at the WWN edge of a 3D relief featuring two 2D appendixes pointing NNE and
305 WWN. The ASS station shows an amplification at 3.5 Hz, polarized at 25°, perpendicularly to the main axis
306 of the ridge. In Ref. [22] the ASS station is indicated in T3 class. The topographic classification map of this

study (Figure 9d) reproduces the morphological features described in Ref. [22], with a T3-T4 class for the WWN edge of the 3D relief.

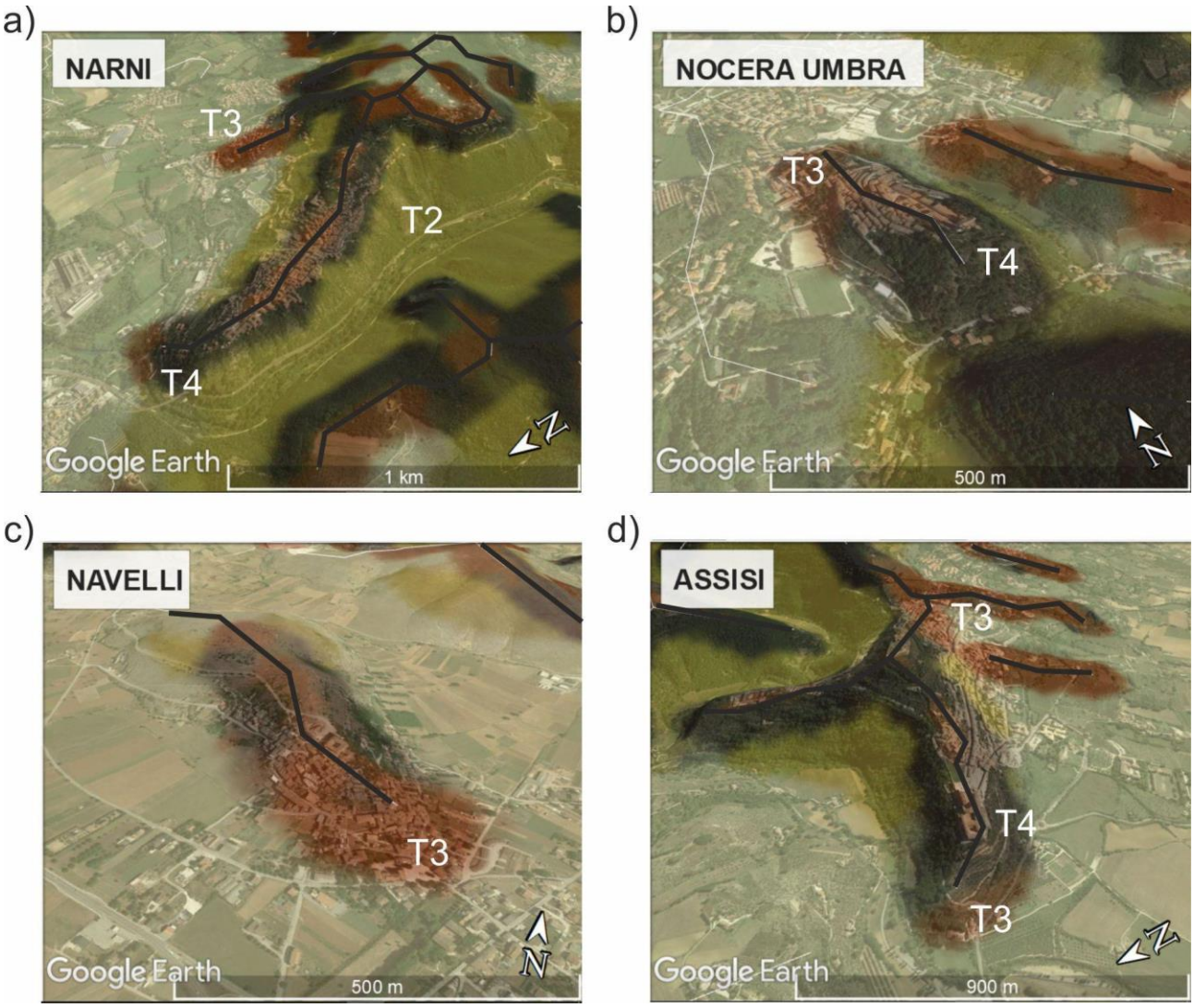

Figure 9. 3D view of the topographic classification map. Narni (a), Nocera Umbra (b), Navelli (c), and Assisi (d). The ridge lines are reported as black solid lines. The legend for color scale is the same as Figure 6.

5. Conclusions

The paper describes a GIS procedure for the topographic classification of a DEM, according to the NTC18 seismic code. The resulting map, with the topographic classification of Italy, is provided in the electronic supplement.

319 The GIS procedure is easily replicable: it makes use of (i) TinItaly high-resolution DEMs, (ii) the ridges
320 identification with the Topographic Position Index (TPI; [35]), and (iii) slope angle and elevation differences
321 calculated with built-in ESRI ArcGIS functions. The procedure allows to univocally classify the Italian
322 territory and improves previous studies [24], where the classification was only performed in the neighbourhood
323 of a single accelerometric station. Moreover, the results of this study do not need a manual revision, usually
324 performed on Google Earth [48, 49, 38]. In this case, not applying quantitative and systematic morphological
325 analyses based on digital elevation models, the topographic classification is affected by a certain level of
326 subjectivity, related to the point of view, and to the complex geomorphology of the site. The overall check
327 between the topographic map and the case studies reported in this work indicates a satisfactory representation
328 of the morphological features and a correct classification of the sites. In case of mismatch, the proposed
329 classification is generally conservative.
330 The statistics computed on the topographic classification map show that one third of the Italian territory is
331 characterized by sites with possible topographic amplification (i.e., T2, T3 and T4 classes, Table 1). In
332 particular, following the NTC18 and EC8 seismic codes, 25% of Italian territory is characterized by a
333 topographic amplification factor of 1.2 (T2 and T3 classes), whereas 12% of the country area presents a
334 topographic amplification factor of 1.4 (T4 class). The NTC18 prescribes the applicability of the topographic
335 coefficients in case of "simple" configurations, but the criteria to discriminate between "simple" and
336 "complex" are not specified and, for this reason, the applicability of the coefficients could be debated. Here
337 we propose the application to the entire Italian territory, extending the classification prescribed in seismic
338 codes for "simple" 2D relief configurations to all 3D geomorphological settings. The statistics computed on
339 the 15332 Italian localities in DBMI [32] support the effectiveness of this extrapolation from 2D to 3D, but do
340 not prove the existence of topographic amplification effects. Based on the topographic classification proposed
341 in this study, about 40% of the localities that experienced the highest macroseismic intensities (*Imax* >6) are
342 potentially affected by topographic amplification (T2-T4 classes). The impact of the topographic amplification
343 (Table 1) on the hazard map [30], calculated as PGA for a return period of 475 years and soil category A
344 (NTC18), is shown in Figure 10. Being the topographic amplification period-independent according to NTC18
345 (Table 1), the effects are the same at all spectral periods.

The map of the topographic classification of Italy can be used for both scientific and application purposes. In this regard, the topographic classification map may be used for the characterization of seismic stations, and may support the identification of sites with systematic topographic effects. The map is also useful for the selection of accelerometric time histories that meet the spectrum-compatibility requirement indicated in the Italian (NTC18) and European (EC8) seismic codes. In the latter case, it allows selecting those stations in T1 class, whose recordings are not affected by topographic amplification. Moreover, the proposed map may guide future investigations of T2, T3 and T4 sites, in particular to study the period-dependent topographic amplifications, as opposed to the constant amplification factors provided in NTC18 and EC8 seismic codes.

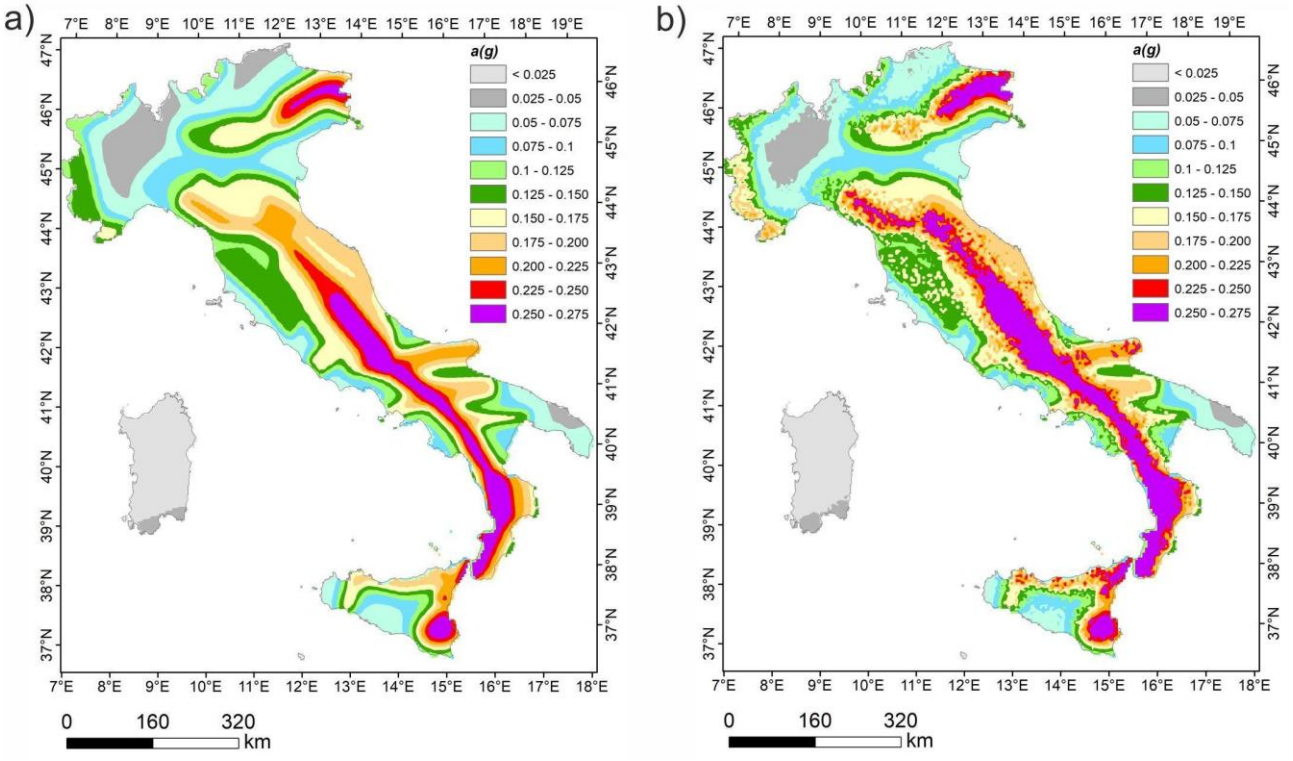

Figure 10: a) probabilistic seismic hazard map for PGA, soil class A and topographic class T1 (return period of 475 years), as in Ref. [30]; b) application of topographic amplification factors according to the classification shown in Figure 6.

Acknowledgment

The study has partially benefited from funding provided by the Italian Presidenza del Consiglio dei Ministri–Dipartimento della Protezione Civile (DPC)—Agreement B2, DPC-INGV. This paper does not necessarily represent DPC official opinions and policies.

CRediT authorship contribution statement

Claudia Mascandola: Conceptualization, Methodology, Software, Writing - original draft, Writing - review & editing, Data curation, Formal analysis. **Lucia Luzi:** Conceptualization, Methodology, Software, Writing - original draft, Writing - review & editing, Data curation, Formal analysis. **Chiara Felicetta:** Writing - original draft, Writing - review & editing, Data curation, Formal analysis. **Francesca Pacor:** Writing - original draft, Writing - review & editing, Data curation, Formal analysis.

References

[1] Boore, D. M. (1972). A note on the effect of simple topography on seismic SH waves, Bull. Seismol. Soc. Am. 62, 275–284.

[2] Bard, P. Y. (1982). Diffracted waves and displacement fields over two dimensional elevated topographies, Geophys. J. Int. 71, 731–760.

[3] Panizza, M. (1991). Geomorphology and seismic risk. Earth-Sci Rev; 31:11–20.

[4] Paolucci, R. (2002). Amplification of earthquake ground motion by steep topographic irregularities. Earthq. Eng. Struct. Dyn.; 31:1831–53.

[5] Griffiths, D.W., and Bollinger, G.A. (1979). The effect of Appalachian Mountain topography on seismic waves. Bull. Seism. Soc. Am.; 69:1081–105.

[6] Kawase, H, and Aki, K. (1990). Topography effect at the critical SV-wave incidence: possible explanation of damage pattern by the Whittier Narrows, California, earthquake of 1 October 1987. Bull. Seism. Soc. Am.; 80:1–22.

388 [7] Marsan, P, Milana, G, Pugliese, A, and Sanò, T. (2000). Local amplification effects recorded by a local
389 strong motion network during the 1997 Umbria-Marche earthquake. In: Proceedings of 12th world conference
390 on earthquake engineering, paper no. 1046. Auckland, New Zealand.

391 [8] Marra, F., Azzara, R., Bellucci, F., Caserta, A., Cultrera, G., Mele, B., Palombo, B., Rovelli, A., and
392 Boschi, E. (2000). Large amplification of ground motion at rock sites within a fault zone in Nocera Umbra
393 (central Italy). J Seismol.;4:543–54.

394 [9] Cara, F., Rovelli, A., Di Giulio, G., Marra, F., Braun, T., Cultrera, G., Azzara R., and Boschi E.(2005).
395 The role of site effects on the intensity anomaly of San Giuliano di Puglia inferred from aftershocks of the
396 Molise, Central Southern Italy, sequence, Bull. Seism. Soc. Am.;95:1457–68.

397 [10] Massa, M., Lovati, S., D'Alema, E., Ferretti, G., and Bakavoli, M. (2010). An experimental approach for
398 estimating seismic amplification effects at the top of a ridge, and the implication for ground-motion
399 predictions: the case of Narni, Central Italy. Bull. Seism. Soc. Am.; 100(6): 286–301.

400 [11] Buech, F., Davies, T.R., and Pettinga, J.R. (2010). The little red hill seismic experimental study:
401 topographic effects on ground motion at a bedrock-dominated mountain Edifice. Bull. Seism. Soc.
402 Am.;100:2219–29.

403 [12] Marzorati, S., Ladina, C., Falcucci, E., Gori, S., Saroli, M., Ameri, G., and Galadini F. (2011). Site effects
404 on the rock: the case of Castelvecchio Subequo (L'Aquila,central Italy). Bull. Earthq. Eng.;9:841–68.

405 [13] Paolucci, R., Faccioli, E., and Maggio, F. (1999). 3D Response analysis of an instrumented hill at
406 Matsuzaki, Japan, by a spectral method. J. Seismol.;3:191–209.

407 [14] Gazetas, G., Kallou, P.V., and Psarropoulos, P.N. (2002). Topography and soil effects in the Ms 5.9
408 Parnitha (Athens) earthquake: the case of Adámes. Nat. Hazards; 27:133–69.

409 [15] Assimaki, D., Gazetas, G., and Kausel, E.. (2005). Effects of local soil conditions and topographic
410 aggravation seismic motion: parametric investigation and recorded field evidence from the 1999 Athens
411 earthquake. Bull. Seism. Soc. Am.; 95:1059–89.

412 [16] Scandella, L, Davì, M, Paolucci, R, and Pessina, V. (2008). Numerical simulation and Gis mapping of
413 seismic amplification due to topographic effects. In: Proceedings of 31st European Seismological Commission
414 (ESC). Crete, Greece.

415 [17] Faccioli, E. (Eds.) (1986). Elementi Per Una Guida Alle Indagini Di Microzonazione sismica – Progetto
416 finalizzato "Geodinamica", Quaderni de "La ricerca scientifica", n.114, CNR, 7, 72–82, (in Italian).

417 [18] Faccioli, E., Vanini, M., Frassine, L. (2002). "Complex" site effects in earthquake ground motion,
418 including topography. In: Proceedings of 12th European Conference on earthquake engineering. Paperno. 844.

419 [19] Galli, P, and Molin, D. (2004). Macroseismic Survey of the 2002 Molise, Italy, Earthquake and Historical
420 Seismicity of San Giuliano di Puglia. Earthq. Spectra; 20(S1):39–52.

421 [20] Tertulliani, A, Arcoraci, L, Berardi, M, Bernardini, F, Camassi, R, Castellano, C, Del Mese, S., Ercolani,
422 E., Graziani, L., Leschiutta, I., Rossi A., and Vecchi M. (2011). An application of EMS98 in a medium-sized
423 city: the case of L'Aquila (Central Italy) after the April 6, 2009 Mw 6.3 earthquake. Bull. Earthq. Eng; 9:67–
424 80.

425 [21] Gizzi, F.T., Potenza, M.R., and Zotta, C. (2012). 3 November 1980 Irpinia-Basilicata earthquake
426 (Southern Italy): towards a full knowledge of the seismic effects. Bull. Earth. Eng; 10:1109–31.

427 [22] Cauzzi, C., Fäh, D., Pessina, V., Faccioli, E., and Smerzini, C. (2012). Topographic amplification from
428 recorded earthquake data and numerical simulations. In 15th World Conference on Earthquake Engineering.

429 [23] Gallipoli, M. R., Bianca, M., Mucciarelli, M., Parolai, S., and Picozzi, M. (2013). Topographic versus
430 stratigraphic amplification: mismatch between code provisions and observations during the L'Aquila (Italy,
431 2009) sequence. Bull. of Earth. Eng., 11(5), 1325-1336.

[24] Pessina, V., and Fiorini, E. (2014). A GIS procedure for fast topographic characterization of seismic recording stations. Soil Dynamics and Earthquake Engineering, 63, 248-258.

[25] NTC (2018). Ministero delle Infrastrutture e dei Trasporti. Aggiornamento delle Norme Tecniche per le Costruzioni. Part 3.2.2: Categorie di sottosuolo e condizioni topografiche, Gazzetta Ufficiale n. 42 del 20 febbraio 2018 (in Italian).

[26] CEN (Comite Europe en de Normalisation), 2004. Eurocode 8. Design Provisions for Earthquake Resistance of Structures—Part 5: Foundations, Retaining Structures and Geotechnical Aspects. ENV 1998-5, CEN European Committee for Standardisation, Brussels, 1994.

[27] NTC (2008). Ministero delle Infrastrutture e dei Trasporti. Nuove Norme Tecniche per le Costruzioni. Part 3: Categorie di sottosuolo e condizioni topografiche, Gazzetta Ufficiale, no. 29, del 4 febbraio 2008 (in Italian).

[28] Luzi, L., Hailemikael, S., Bindi, D., Pacor, F., Mele, F., and Sabetta, F. (2008). ITACA (ITalian ACcelerometric Archive): A Web Portal for the Dissemination of Italian Strong-motion Data, Seismological Research Letters, 79(5), 716–722.

[29] Pacor, F., Paolucci, R., Luzi, L., Sabetta, F., Spinelli, A., Gorini, A., Nicoletti, M., Marcucci, S., Filippi, L., and Dolce M. (2011), Overview of the Italian strong motion database ITACA 1.0, Bull. Earth. Eng, 9(6), 1723–1739.

[30] MPS Working Group (2004). Redazione della mappa di pericolosità sismica prevista dall'Ordinanza PCM del 20 marzo 2003, Rapporto Conclusivo per il Dipartimento della Protezione Civile (in Italian).

[31] Stucchi, M., C. Meletti, V. Montaldo, H. Crowley, G. M. Calvi, and E. Boschi (2011). Seismic hazard assessment (2003–2009) for the Italian building code, Bull. Seismol. Soc. Am. 101, no. 4, 1885–1911.

[32] Locati, M., Camassi, R., Rovida, A., Ercolani, E., Bernardini, F., Castelli, V., Caracciolo, C.H., Tertulliani, A., Rossi, A., Azzaro, R., D'Amico, S., Conte, S., Rocchetti, E., Antonucci, A. (2019). Database

455 Macrosismico Italiano (DBMI15), versione 2.0. Istituto Nazionale di Geofisica e Vulcanologia (INGV).
456 https://doi.org/10.13127/DBMI/DBMI15.2

457 [33] D'Amico, M., Felicetta, C., Russo, E., Sgobba, S., Lanzano, G., Pacor, F., and Luzi, L. (2020). Italian
458 Accelerometric Archive v 3.1 - Istituto Nazionale di Geofisica e Vulcanologia, Dipartimento della Protezione
459 Civile Nazionale. doi: 10.13127/itaca.3.1

460 [34] Tarquini, S., Isola, I., Favalli, M., Mazzarini, F. ,Bisson, M., Pareschi, M.T., and Boschi, E. (2007).
461 TINITALY/01: a new triangular irregular network of Italy. Annals of Geophysics 50,407–425.

462 [35] Weiss, A. (2001). Topographic position and landform analysis. Poster presentation, ESRI Users
463 Conference, San Diego, CA.

464 [36] Burrough, P. A., and McDonell, R. A., (1998). Principles of Geographical Information Systems (Oxford
465 University Press, New York), 190 pp.

466 [37] Jenness, J., Brost, B., and Beier, P. (2013). Land facet corridor designer. USDA forest service rocky
467 mountain research station.

468 [38] Mascandola, C., Massa, M., Lovati, S., and Augliera, P. (2018). The site characterization scheme of the
469 INGV strong motion database (ISMD): Overview and site classification. Seism. Res. Lett., 89(1), 86-98.

470 [39] Zhan, C. (1993). A Hybrid Line Thinning Approach. Proceedings Auto-Carto 11, Minneapolis, pp. 396-
471 405.

472 [40] OPCM n. 3519 (2006): criteri generali per l'individuazione delle zone sismiche e per la formazione e
473 l'aggiornamento degli elenchi delle stesse zone; Gazzetta Ufficiale n. 108 dell'11 maggio 2006 (in Italian).

474 [41] ISTAT, 2011. 154° Censimento della Popolazione e delle Abitazioni. http://www.istat.it/it/censimento-
475 popolazione/censimento-popolazione-2011.

476 [42] Sieberg, A. (1930). The earthquake geology (Geologie der Erdbeben). Handbuch der Geophysik
477 2(4):550–555 (in German).

[43] Caserta, A., Bellucci, F., Cultrera, G., Donati, S., Marra, F., Mele, G., Palombo, B. and Rovelli, A. (2000). Study of site effects in the area of Nocera Umbra (Central Italy) during the 1997 Umbria-Marche seismic sequence, J. Seismol., 4, 555–565.

[44] Donati, S., Marra, F. and Rovelli, A. (2001). Damage and ground shaking in the town of Nocera Umbra during Umbria-Marche, central Italy, earthquakes: the special effect of a fault zone, Bull. seism. Soc. Am., 91, 511–519.

[45] Pischiutta, M., Cultrera, G., Caserta, A., Luzi, L., and Rovelli, A. (2010). Topographic effects on the hill of Nocera Umbra, central Italy. Geophysical Journal International, 182(2), 977-987.

[46] Lovati, S., Bakavoli, M. K. H., Massa, M., Ferretti, G., Pacor, F., Paolucci, R., Haghshenas E., and Kamalian, M. (2011). Estimation of topographical effects at Narni ridge (Central Italy): comparisons between experimental results and numerical modelling. Bull. of Earth. Eng., 9(6), 1987-2005.

[47] Pischiutta, M., Cianfarra, P., Salvini, F., Cara, F., and Vannoli, P. (2018). A systematic analysis of directional site effects at stations of the Italian seismic network to test the role of local topography. Geophysical Journal International, 214(1), 635-650.

[48] Pessina, V. (2010). Appendix E. EC8 subsoil and topographic classification of ITACA stations Deliverable D10, Project S4 The Italian strong motion database. http://esse4.mi.ingv.it/files/images/stories/d10_appendix%20e.pdf

[49] Di Capua, G., Lanzo, G., Pessina, V., Peppoloni, S., and Scasserra, G. (2011). The recording stations of the Italian strong motion network: Geological information and site classification. Bulletin of Earthquake Engineering, 9(6), 1779-1796.

A GIS procedure for the topographic classification of Italy, according to the seismic code provisions

Claudia Mascandola[a*], Lucia Luzi[a], Chiara Felicetta[a], Francesca Pacor[a]

[a] Istituto Nazionale di Geofisica e Vulcanologia, Sezione di Milano, Milano, Italy

[*] Corresponding author. E-mail address: claudia.mascandola@ingv.it

Abstract

In this study we present a procedure for the topographic classification of Italy, taking advantage of existing high-resolution digital elevation models (DEM), with the support of routines embedded in Geographic Information Systems. The proposed method is based on morphometric analyses of a DEM, allowing for hilltop ridge detection, slope computation, identification of reliefs with potential topographic site effects, and topographic classification according to the indications of the current European and Italian seismic codes. The developed procedure can be applied worldwide and has a potential engineering interest for a fast and accurate topographic classification of a site, for both scientific and application purposes. The topographic classification of Italy is tested on several well-known cases of topographic amplification and it is adopted for the topographic classification of Italian accelerometric stations.

Keywords: DEM, Topographic classification, EC8, NTC18, GIS, Morphometric analyses

Supplementary data. The topographic classification of Italy is available in the electronic supplement.

1. Introduction

One of the possible causes of damage during earthquakes is the seismic waves amplification due to topographic irregularities. The reasons for topographic amplification may be several: the resonance of the whole relief when the incident seismic field has a predominant wavelength comparable to the horizontal width of the

mountain [1]; the focusing of seismic waves near the crest because of the reflection on a free surface and/or the interaction between incident and diffracted waves [2]. Moreover, topographic seismic amplification is considered as one of the possible causes of triggers of earthquake induced phenomena, like landslides, which represent one of the major causes of earthquake-related devastation (e.g. Refs. [3,4]). Several studies over the last four decades have discussed the effects of surface topography on seismic ground motions from instrumental investigations [5-12] and numerical models [13, 14, 4, 15, 16]. Relevant macroseismic case histories are reported by several authors [17, 18, 4, 19, 20, 21]. The proper assessment of topographic amplification is of key importance in the European context, where a broad range of exposure levels to earthquake hazard is encompassed [18] and many small towns are located at the top of isolated steep cliffs. Such unfavourable conditions often come together with high vulnerability of the buildings and the susceptibility to slope sliding [4]. Therefore, the topographic amplification, even if generally do not exceed the stratigraphic one (e.g. Refs. [4, 22, 23, 24]), plays a significant role in seismic design, microzonation studies and hazard analyses.

The current Italian (NTC, 2018; hereinafter NTC18 [25]) and European (CEN, 2004; hereinafter EC8 [26]) seismic codes prescribe frequency-independent amplification factors not larger than 40%, based on the height and the slope of simple 2D relief configurations. The approach, introduced in the EC8, was further adopted by NTC (2008) [27] and the current NTC18, where four classes of topographic amplification are explicitly defined, as listed in Table 1. These categories refer to bidimensional configurations, such as elongated crests and ridges, and must be considered only when their height is greater than 30m.

Table 1: Topographic amplification factors prescribed by Italian seismic code (NTC18).

Topographic Class	Description	Amplification factor
T1	Flat surface, isolated slopes and cliffs with average slope angle $i \leq 15^\circ$	1
T2	Slopes with average slope angle $i > 15°$	1.2
T3	Relief with ridge width much smaller than the base and average slope angle $15° < i \leq 30^\circ$	1.2
T4	Relief with ridge width much smaller than the base and average slope angle $i > 30°$	1.4

Following the classification of the Italian seismic code, Ref. [24] first implemented a procedure for the topographic characterization of seismic recording stations archived in ITACA 2.0 database (Italian Accelerometric Archive, http://itaca20.mi.ingv.it/ItacaNet_20/; [28, 29]). The procedure is based on morphometric analyses of high-resolution digital elevation models (DEMs), with the support of Geographic Information Systems (GIS). In the specific, the procedure computes the slope and ridge layers from DEM, besides different statistical indicators (i.e., maximum, minimum, sum, and mean) within a circular buffer area around each recording station. These statistical indicators are combined to provide both a slope and a ridge index that are further matched to define the topographic classification of the seismic station. However, some combinations of the indices do not permit a univocal topographic classification because their arrangement may lead to different topographic classes (in that case the site is not classified). Moreover, the procedure implemented for the ridge detection is not straightforward and implies several noise removal steps to enhance significant features and remove small topographic irregularities. Since the procedure is applied to the surroundings of each seismic station, it needs to be run each time a new seismic station is added to the database. These downsides led to the development of a new GIS-based procedure for topographic classification of the whole Italian territory. However, the NTC18 prescribes the applicability of the topographic coefficients in case of "simple" configurations, but the criteria to discriminate between "simple" and "complex" are not specified and, for this reason, the applicability of the coefficients could be debated.

In this study, we propose a step-like procedure and provide some statistics of the resulting map, correlating it to the probabilistic seismic hazard [30, 31], the macroseismic intensity data in DBMI15 [32], and the seismic stations in the Italian Accelerometric Archive 3.1 (ITACA 3.1; http://itaca.mi.ingv.it/ItacaNet_31/#/home; [33]). The topographic classification is tested at several sites, where topographic amplification has been observed. Finally, based on the proposed classification, we evaluate the impact of the topographic amplification factors (Table 1), on the probabilistic seismic hazard map calculated for Peak Ground Acceleration (PGA), a return period of 475 years, and stiff soil i.e. soil class EC8-A [30].

2. Method

Digital elevation models (DEMs) are fundamental in environmental and morphological analyses. In this study, the topographic classification is applied to the so called *TinItaly DEM* [34], created for the whole Italian territory as a triangular irregular network (TIN), and converted into grid format of 10m cell size, according to a tiled structure composed of 193, 50-km side square elements. Ref. [34] carried out a comprehensive assessment of the accuracy of the TinItaly DEM, finding a root mean square error in elevation (RMSEz) between 0.8 and 6.0 m. For our analysis, we select the TinItaly DEM since, to date, it is the model with the highest resolution, freely available for scientific purposes for the whole Italian territory.

The morphological analyses applied on the DEM are summarized in Figure 1 and described in detail in the following subparagraphs. Starting from DEM (Figure 1, step 1), the slope angle is computed (step 2) along with the Topographic Position Index (TPI; [35], step 3) and the elevation range (maximum minus minimum elevation value in a moving window), applying a threshold height of 30 m (H30) and 60 m (H60), respectively (step 4). Since the positive TPI values allow detecting the ridge zones, an empirical threshold of 5 m is adopted to discriminate between ridges (ridge is assigned 1) and non-ridges (ridge is assigned 0). Considering the slope and TPI values, a first discrimination of topographic classes can be performed (Figure 1). Whereas T1 and T2 sites are on slopes (ridge = 0), T3 and T4 sites should be on ridges (ridge = 1). Therefore, T1 and T2 categories can be identified by the combination of ridge = 0, and slope angle $< 15°$ or $\geq 15°$, respectively (step 6); T3 and T4 classes can be identified by ridge = 1 (Figure 1, step 5), on reliefs with difference in height > 30 m. To further discriminate between T3 and T4 classes, the H60 map is considered. When H60 = 1 (elevation range

H is between 30 and 60 m) the site is in class T3 (step 6). In the following, the step-like procedure applied to the TinItaly DEM is described in detail, indicating the ESRI ArcGis (www.esri.com) tools adopted for the morphological analyses.

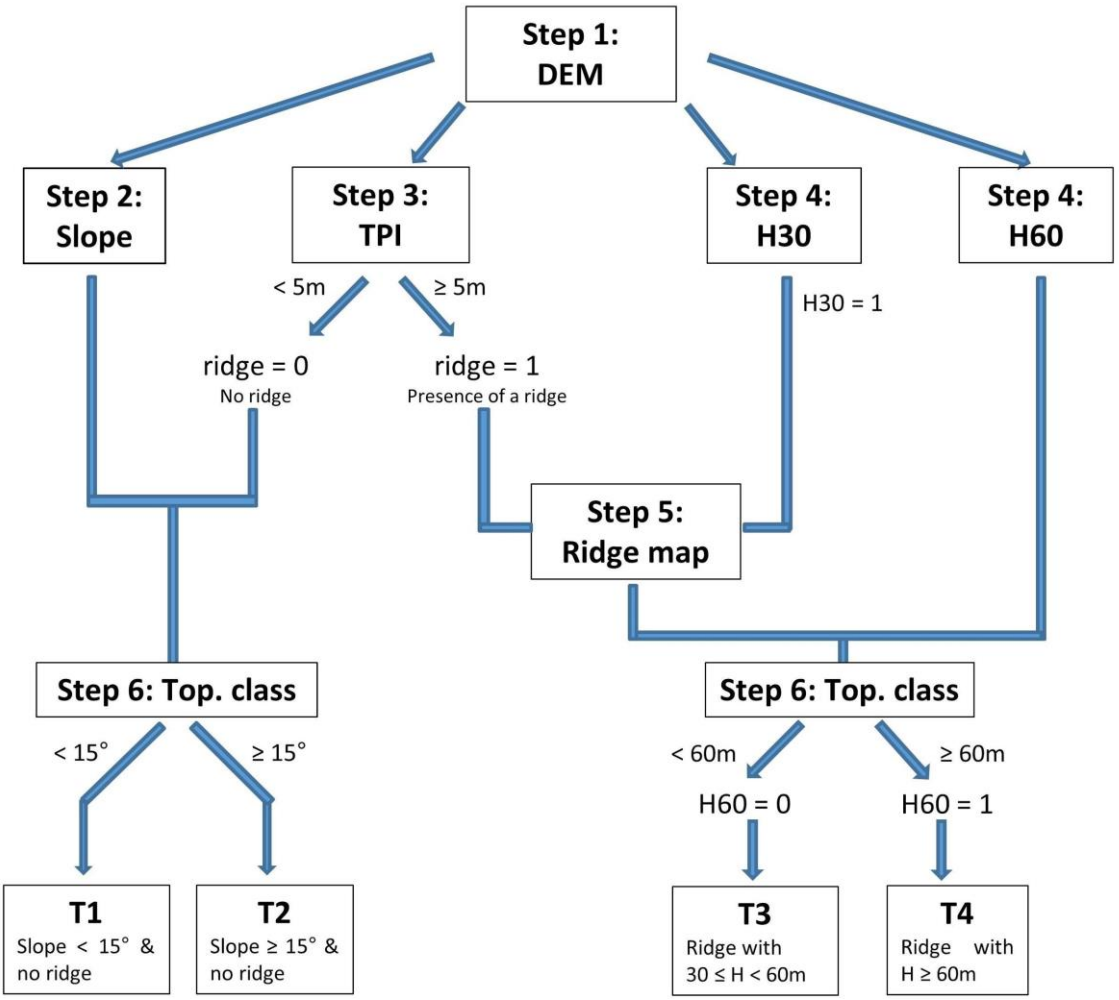

Figure 1: Workflow for topographic classification.

Step 1: preliminary DEM processing

To improve the computation time and data handling, the 193 TinItaly DEM tiles are resampled with a 40 m resolution. Afterwards, the DEM tiles are merged to obtain a unique map for the Italian territory. Finally, to remove minor irregularities, a smoothing is performed by applying a mean algorithm with a 3x3 moving window (e.g. *Focal Statistics* tool in ESRI ArcGis), as shown in Figure 2a for a sample area in central Apennines.

Step 2: computation of topographic slope

To compute the slope angle, we use the *Slope* function implemented on ESRI ArcGis (Figure 2b). The slope is computed in degree units in a 3 by 3 cell neighborhood (i.e., moving window) on the smoothed DEM, considering the planar method with the average maximum technique [36]. The slope is measured as the maximum rate of change in value from a cell to its immediate neighbors. The calculation is performed on a projected flat plane using a 2D Cartesian coordinate system. The processed cell is judged reliable if the computation is performed on at least seven cells in the 3 by 3 neighborhood.

Step 3: ridge extraction

For the ridge detection, we adopt the Topographic Position Index (TPI) algorithm proposed by Ref. [35]. This algorithm is implemented in the *Land Facet Analysis* toolbox [37] in ESRI ArcGis. The TPI is defined as a difference between the actual value of the elevation H at given location [x, y] and mean elevation of the neighboring area A:

$$TPI(x,y) = H(x,y) - \int_A H(x,y)\partial S \,/\, \int_A \partial S \qquad \text{Eq. (1)}$$

The area A should be centered at the point [x, y]. Both the size and the shape of the neighboring area have to be defined in advance, depending on the specific application. In general, there is no constraint on both values. The TPIs reflect the differences between the elevation in a particular cell and the mean elevation of the surrounding cells: positive values mean the cell is higher than its surroundings, while negative values mean it is lower. Therefore, high positive values of TPI characterize ridgetops and hilltops, while negative values define basins or valley bottoms. TPI values close to zero indicate flat or mid-slope areas. This kind of analysis strictly depends on the scale used to count the surrounding cells. To set the interval for the TPI analysis, we carry out some tests, considering different radii (i.e. 300 m, 500 m and 800 m). For the Italian case, a neighborhood circle with a radius of 500 m is adopted, since it allows better discriminating the ridges out of the main reliefs, while ignoring the minor deflections [38]. The ridge zones are obtained from the TPI map (*Raster Calculator* tool) considering a threshold value equal to 5. The output is a binary raster that takes the value 1 when TPI > 5 and 0 otherwise (Figure 2c). Since TPI units are in meters, a TPI value of 5 means that

this particular cell is 5 m higher than the average elevation of its neighborhood (i.e., a radius of 500 m). The TPI threshold is selected empirically. A lower threshold (down to 1) does not significantly affect the final results. The ridgelines are retrieved by applying a thinning function (*Thin* tool) that thins rasterized linear features by reducing the number of cells representing the width of the features [39], as shown in Figure 2d.

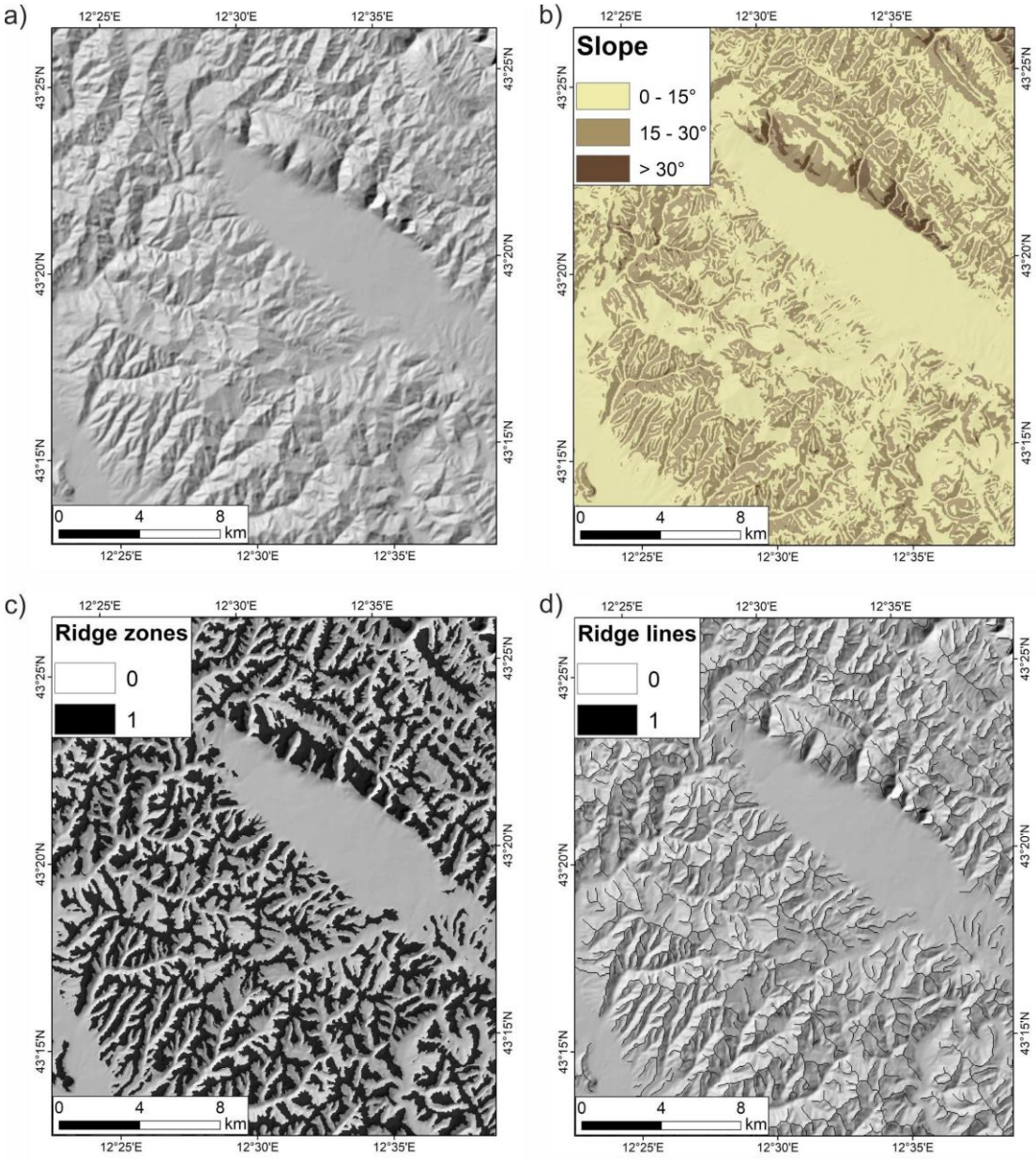

Figure 2: Extraction for an area of the Central Apennines of a) DEM, represented as hillshade; b) topographic slope; c) ridge zones setting TPI > 5; and d) ridge lines after thinning.

Step 4: detection of the difference in height to extract topographic categories T3 and T4

In the EC8 and NTC18 seismic codes, reliefs higher than 30 m are considered to have potential topographic site effects (i.e., T3 or T4 topographic classes in NTC18). To individuate these reliefs, we compute the

elevation range, i.e., maximum minus minimum elevation value, in 5x5 cells moving windows (Figure 3a; *Focal Statistics* tool). Considering that the DEM cell size is 40 m, the maximum and minimum semi-transverse axis of a relief spanned by a 5x5 moving window is 113 m (e.g. $80 \cdot \sqrt{2}$m), as exemplified by the dark grey line in Figure 3, and 40 m (light grey line in Figure 3), respectively. Considering a threshold difference in height of 30 m (condition for topographic amplification), we obtain the slope angle interval, which ranges between 14° and 37° (Figure 3b,c), thus including both T3 and T4 classes. To discriminate class T4, we consider the map representing the difference in height of 60 m that individuates the slope angles in the interval 27°-56° (Figure 3d,e), including T4 sites (i.e, ridges with height greater than 30 m and average slope angle $i >$ 30°). In the following sections, the elevation range computed with a threshold height of 30 m is indicated as H30; whereas the elevation range computed with a threshold height of 60 m is indicated as H60 (Figure 4).

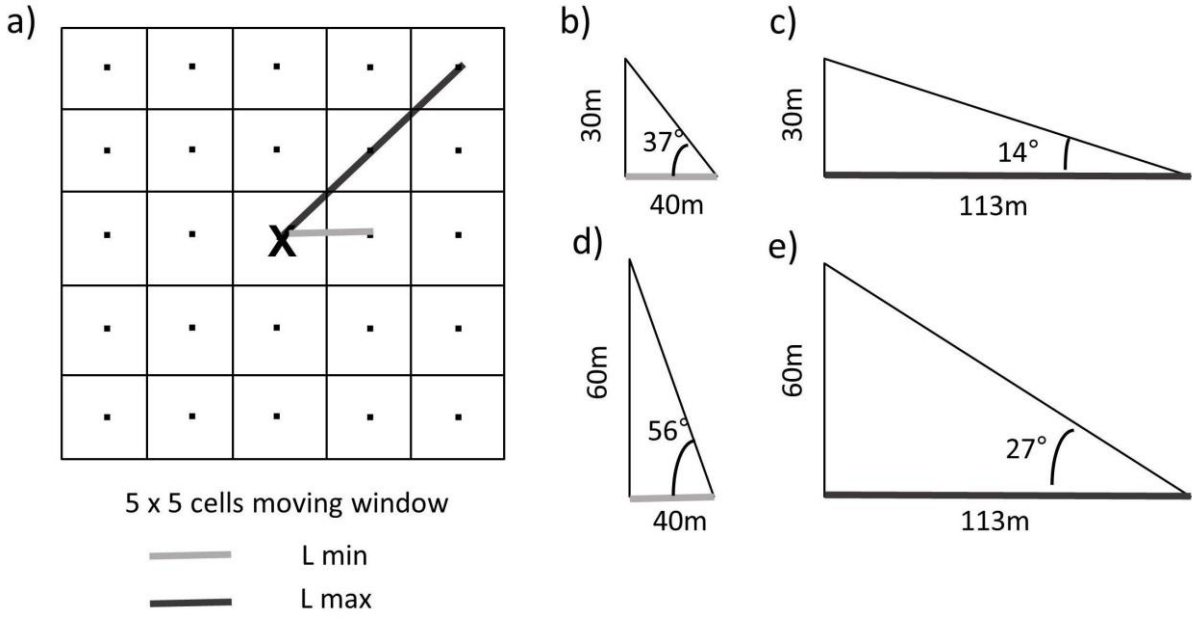

Figure 3: Trigonometry applied to H30 and H60 maps. a) 5x5 cells moving window with the smaller (light grey line) and larger (dark grey line) semi-transverse axis spanned in the moving window. b)-c) maximum and minimum slope angles, considering a difference in height of 30 m, d)-e) maximum and minimum slope angles considering a difference in height of 60 m.

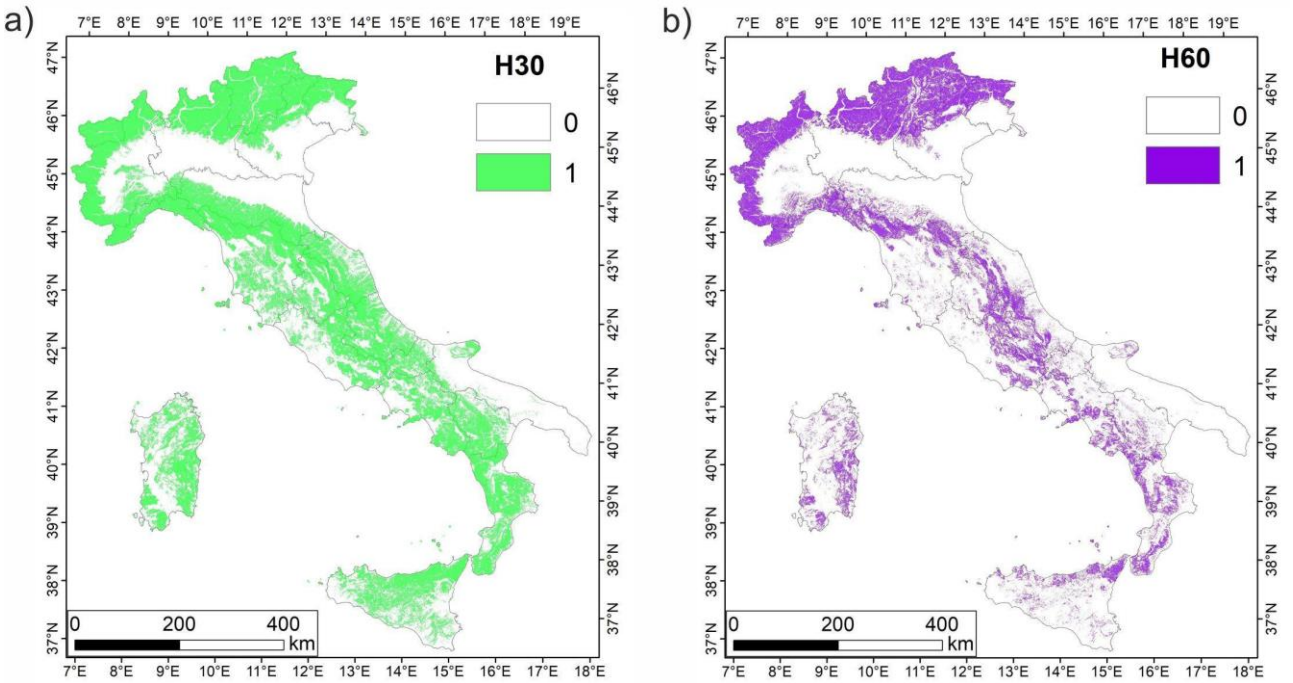

Figure 4: Map of a) difference in height of 30 m (H30) and b) 60 m (H60) for the Italian territory.

Step 5: identification of T3 and T4 topographic categories

After the identification of the difference in height to extract T3 and T4 topographic categories, the ridge lines of the corresponding reliefs can be obtained by overlapping the ridge line map (evaluated in step 3) and the H30 map (evaluated in step 4) (*Raster calculator* tool, imposing H30 =1 & ridge lines =1), as shown in Figure 5a. To identify the sparse groups of points (< 5 cells), the *Region Group* tool is combined with the *Set Null* operator. The *Region Group* counts the number of grouped cells within an 8-cells neighborhood (excluding 0 values), and the *Set Null* sets to null the cell values for counts less than 5. The sparse groups of points are finally removed with the *Nibble* operator that allows filtering of the ridge line raster. Finally, the extracted ridges are dilated (3 cells per side), using the *ArcScan* extension (Figure 5b). Being the raster cell size 40 m, the ridge lines are dilated by 120 m per side to approximate the semi-transverse axis of a relief with a minimum 30 m of difference in height and a consequent minimum slope angle of 15°, which are the thresholds for topographic amplification according to NTC18 and EC8 seismic codes (see Figure 3c as an example). In this sense, the 120 m per side is conservative because it may include the whole relief down to the base.

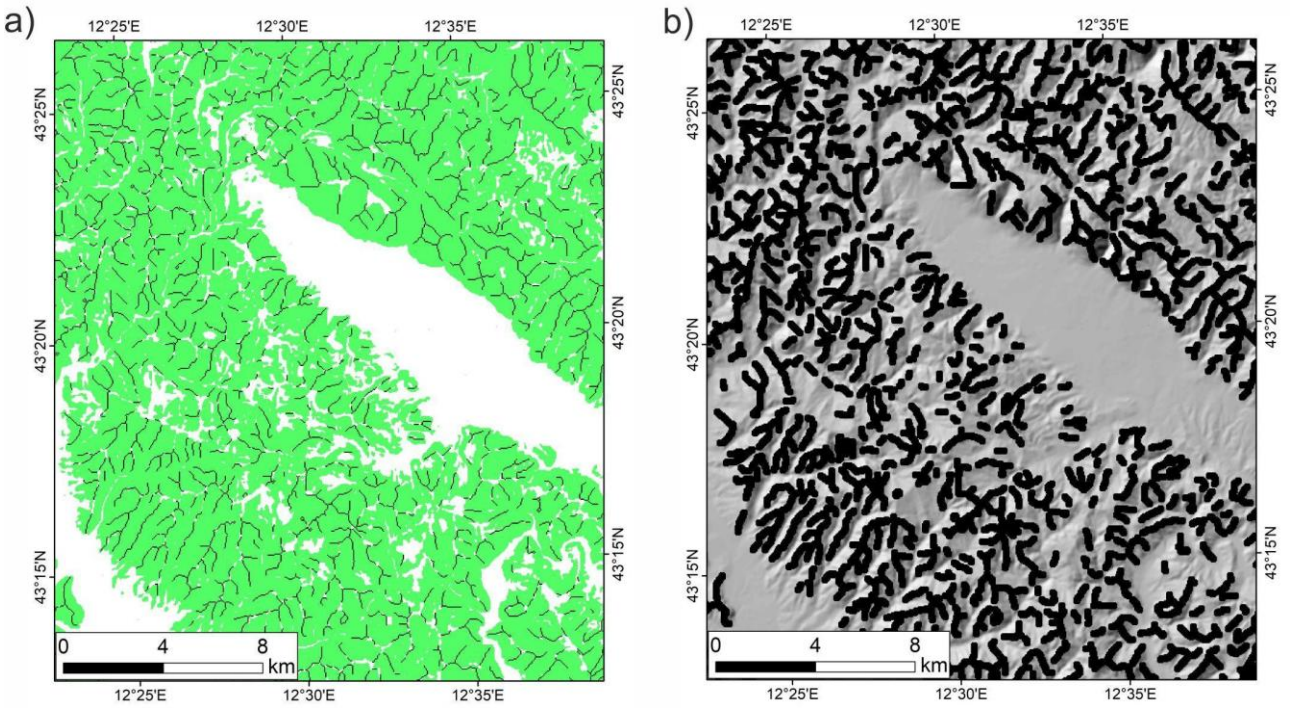

Figure 5: a) intersection between ridge line map (black lines) and H30 map; b) ridge map on DEM represented as hillshade.

Step 6: topographic classification

Once the identification of the morphological parameters is performed, the final topographic classification is obtained by combining the following maps:

1. slope angles (*slope* map);
2. ridges of reliefs with potential topographic amplification (*ridge* map);
3. reliefs with average slope angle $i > 30°$ (*H60* map);

as reported in Table 2 (*Raster calculator* tool). The final topographic classification is reported in Figure 6 and provided in the electronic supplement.

Table 2: Topographic classification (NTC18), based on the proposed GIS-procedure.

Condition	Class	Description
ridge = 0 & slope < 15°	T1	slope with average slope angle $i < 15°$
ridge = 0 & slope ≥ 15°	T2	slope with average slope angle $i \geq 15°$
ridge = 1 & H60 = 0	T3	ridge with difference in height in the range 30-60 m (i.e. base angle ≤ 30°)
ridge = 1 & H60 = 1	T4	ridge with difference in height > 60 m (i.e. base angle > 30°)

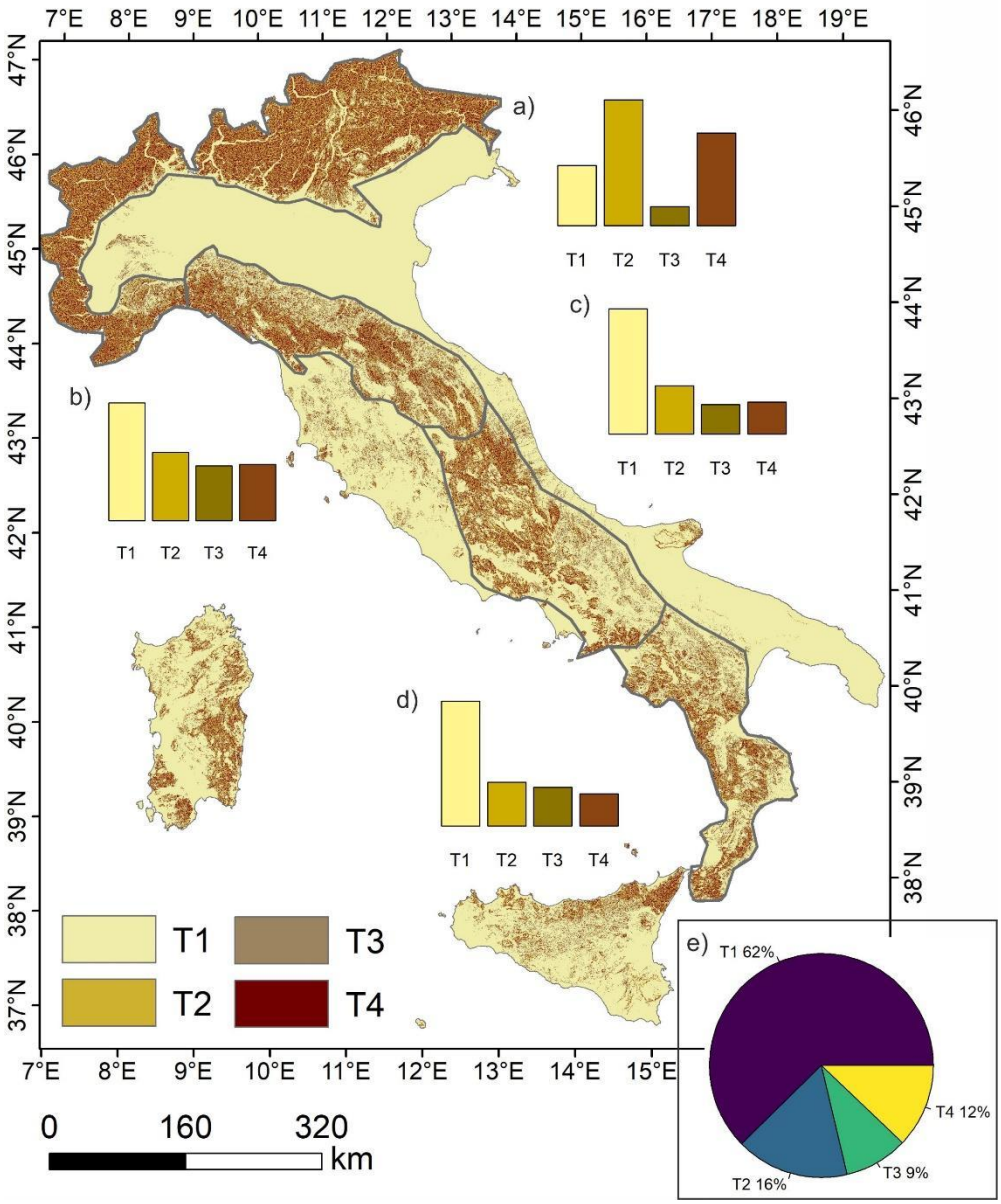

Figure 6: Topographic classification of Italy according to the current Italian seismic code (NTC18), obtained following the proposed procedure. The histograms of the topographic classes are reported for the Alps (a) and the Apennine (b, c, d) mountain chains, in the Northern, Central, and Southern sectors respectively (grey outline). e) Pie chart of topographic classes (T1-T4) for the whole Italian territory. The statistics are computed on a sample of 10,000 random points distributed homogeneously throughout the Italian territory. The count is normalized to the number of points in each sector.

3. Statistics on the topographic classification map

To provide an overview of the topographic classification map in Figure 6, some statistics are computed on a sample of 10,000 random points distributed homogeneously throughout the Italian territory, with a minimum interdistance of 50 m. Figure 6 shows the distribution of the topographic classes for different zones (i.e., Alps and Northern, Central, Southern Apennines). The Alps are characterized by prevalent T2 slopes (42%) and T4 ridges (31%) (Figure 6a), whereas the Apennines are characterized by prevalent T1 slopes (40-50%) with equally distributed T3 and T4 ridges (both are around 15-20%) (Figure 6b, c, d). Most of the Apennines reliefs are concentrated to the North (Figure 6b), where the percentage of T2, T3 and T4 classes is larger (~60%) than in the southern sector of the Apennines (~45%) (Figure 6 c,d). Overall, about one third of the Italian territory is characterized by sites with possible topographic amplification (i.e., T2, T3 and T4 classes in Figure 6e). In detail, 25% of Italian territory is characterized by sites in T2 or T3 (topographic amplification factor of 1.2, Table 1), whereas 12% of the country area is in T4 (topographic amplification factor of 1.4, Table 1) (Figure 6e).

In Figure 7, we show how the proposed topographic classes for the whole Italian territory are distributed with respect to the maximum observed macroseismic intensity (*Imax*, Mercalli-Cancani-Sieberg; [42]) at 15332 Italian localities in DBMI15 [32] and the seismic zones in Ref. [40] (S1-S4). As expected, the localities with the lower *Imax* (Figure 7a) are concentrated in the lower seismic hazard zones (S3 and S4, ag $\leq$ 0.15) of Northern Italy, moving gradually toward the higher seismic hazard zones (S1 and S2, ag > 0.15) of the Central-Southern Apennines for *Imax* > *8* (Figure 7d). When we also consider the topographic classification of this

study, about 40% of the localities with the higher *Imax* (>6) is affected by topographic amplification (T2-T4 classes, Figure 7c-d), in contrast to just about 20% for lower *Imax* (<6) (Figure 7a-b). Moreover, we observe a clusterization of the sites with possible topographic amplification (T2-T4 classes) in Figure 7c, with localities characterized by medium high *Imax* (between 6 and 8), localized in seismic zone 2 (S2: $0.15 < ag \leq 0.25$). These results do not prove the existence of topographic amplification at those sites classified in T2-T4, but the coherency between the topographic classification (T1-T4), the maximum observed microseismic intensity (*Imax)*, and the seismic hazard map, represented by the seismic zones S1-S4.

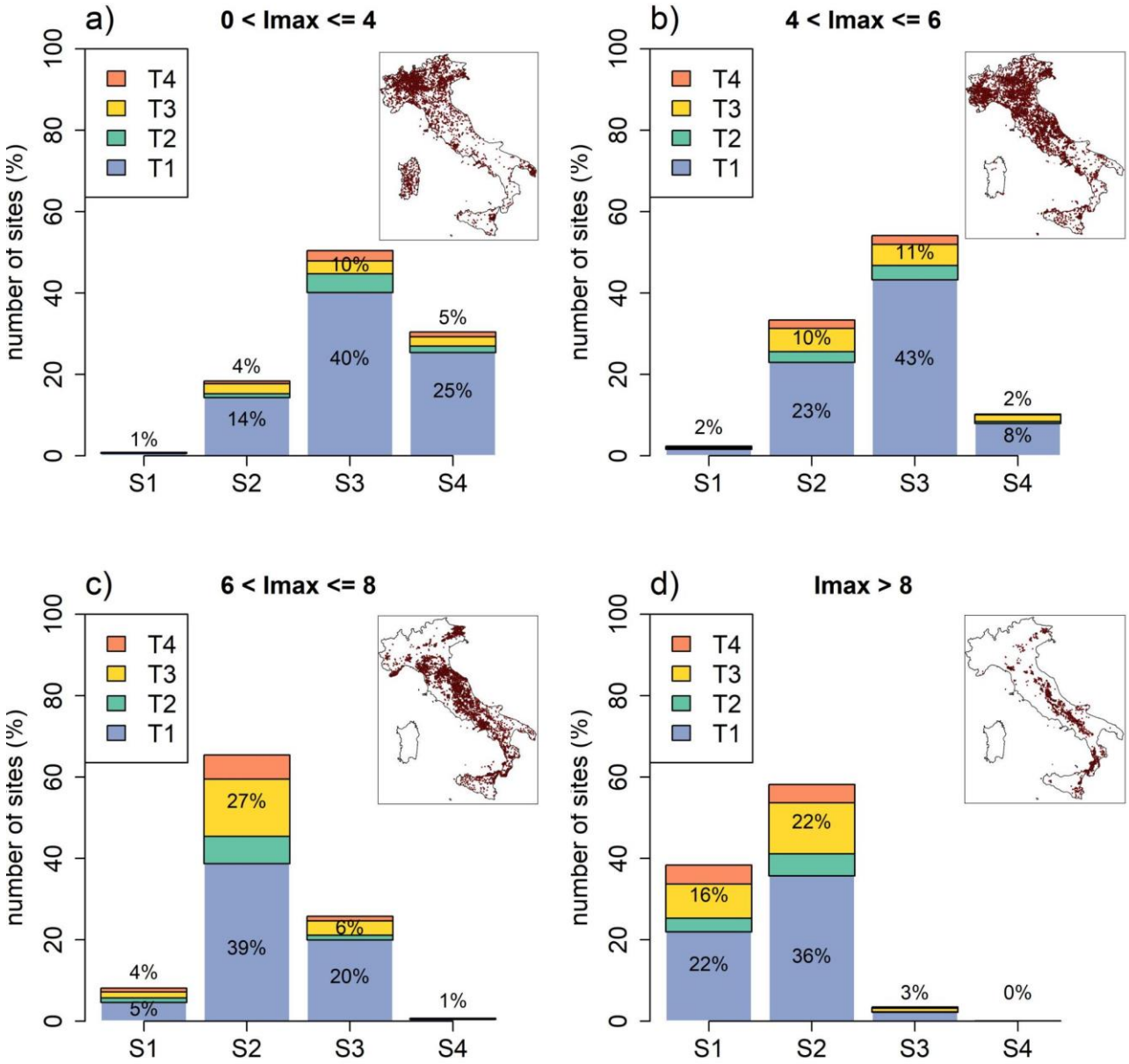

Figure 7: Statistics on the topographic classification of 15332 Italian localities in DBMI15 [32], grouped based on the maximum observed macroseismic intensity at a site (*I max*, Mercalli-Cancani-Sieberg; [42]). a) *I max* $\leq$ 4, b) 4 < *I max* $\leq$ 6, c) 6< *I max* $\leq$ 8, d) *I max* >8. The percentages are normalized to the number of sites in each group. S1-S4 are the seismic zones in Ref. [40], and T1-T4 are the topographic classes in NTC18. The geographic distribution of each dataset in panels a)-d) is reported in the insets.

Finally, we classify the seismic stations archived in the ITACA 3.1 database according to the map in Figure 6. The stations of the Italian Strong Motion Network (RAN; http://ran.protezionecivile.it/IT/index.php) operated by the Department of Civil Protection (IT network code), and of the Italian National Seismic Network (RSN; http://cnt.rm.ingv.it/instruments/network/IV), run by National Institute of Geophysics and Volcanology (IV network code), are considered in Figure 8a and Figure 8b, respectively. The accelerometric sites, classified as T1, reflect the distribution in Figure 6e (62% of Italian territory is in T1); however the percentage of T1 sites in IV and IT networks is quite different (53% versus 68%, respectively, as in Figure 8). Indeed, most seismic stations of the IT network are installed in urban areas for civil protection purposes (Figure 8a), whereas many stations of the IV network are installed outside urban areas for seismic monitoring or scientific purposes (Figure 8b). Among the other topographic classes, both networks have a majority of T3 class for those stations on the Appennine ridges (Figure 8), whereas the T2 and T4 classes are distributed between the Alps and Apennine mountain chains (Figure 8). The percentage of T2 sites in the IT and IV networks is equivalent (~7%), but the percentage of T3 (17% for IT; 26% for IV) and T4 (6% for IT; 12% for IV) sites nearly duplicates moving from IT to IV network (Figure 8).

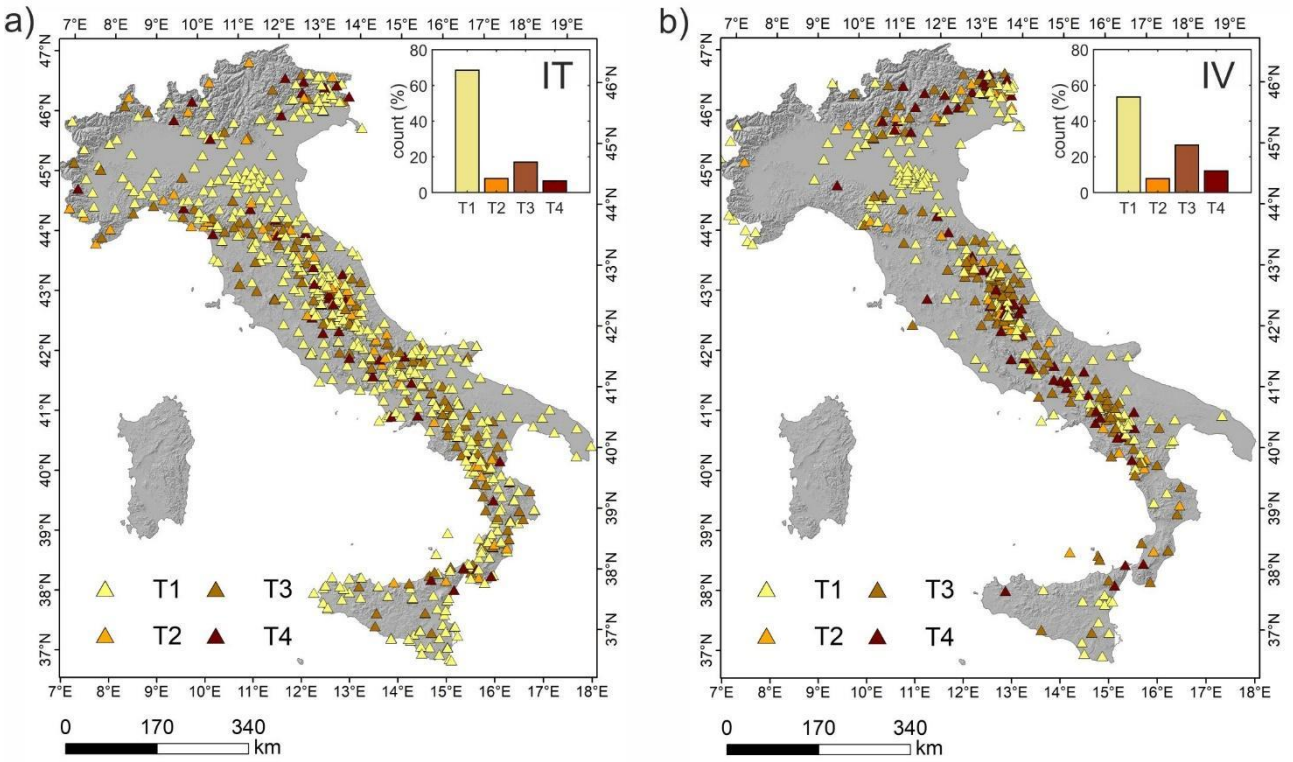

Figure 8: topographic classification for the seismic stations of the ITACA 3.1 database for the RAN network (a), and the RSN network (b). IT: network code of the RAN stations; IV: network code of the RSN stations.

4. Testing of the topographic classification on case studies

The proposed topographic classification is tested at different sites for which topographic amplification is well known (e.g. Refs. [43, 44, 10, 45, 46, 22, 23, 47]). In this study we consider Narni, Navelli, Nocera Umbra, and Assisi (Figure 9).

The seismic amplification of the Narni ridge was investigated through numerical modelling and empirical observations (e.g. Refs. [10, 46]), which proved the dependence of amplification on morphological features. The experimental evidence shows an amplification of the reference motion up to 2.2-3, for the spectral ordinates in the range 0.2-0.3 s (4-5 Hz). The largest amplifications are observed when the direction of the ground motion is perpendicular to the main axis of the ridge. Ref. [10] describe the Narni ridge as 220-m-high, with slopes ranging from 22° to 35°. According to the authors, the topographic class of the Narni ridge is T3

281 at the eastern end, and T4 at the western end, in agreement with the topographic classification of this study
282 (Figure 9a).

283 The Nocera Umbra hill was studied by several authors (e.g. Refs. [43-45]). The historical centre of Nocera
284 Umbra suffered MCS intensity VII–VIII, due to the M_W 5.7 and 6.0 Umbria–Marche earthquakes on 1997,
285 September 26th. The hill is elongated in the NNW–SSE direction, with a maximum height of 574 m a.s.l., and
286 a difference in height equal to 144 m. The northern side of the hill is quite gentle, while the southern one is
287 very steep, therefore the topographic profile along the major axis is asymmetric with a narrow ridge. In
288 contrast, the transverse section is more regular and symmetric, with a base width of about 400 m. Topographic
289 amplification effects are observed at about 3.5 Hz, where the polarization is transversal to the major axis of
290 the hill. The topographic classification map of this study (Figure 9b) reproduces the morphological features
291 described in Ref. [45], with a T3 class at the northern end of the relief, and a T4 class at the southern end.

292 The Navelli ridge was studied by Ref. [23]. The historical centre of Navelli is located along the south-western
293 slope of a NW-SE-trending narrow ridge, which is lithologically characterized by the outcropping crystalline
294 limestones. For this case study, a combination of topographic and stratigraphic amplifications was observed,
295 given a station on a rocky slope (in the historical center of Navelli) and one on a flat alluvial valley (at the base
296 of the hill). The mean slope angle along the historical center is 19° and considering that this morphological
297 ridge is much narrow at the top with respect to its base, the Navelli historical centre can be ascribed to the
298 topographic category T2 [23]. The topographic classification map of this study reproduces the morphological
299 features described in Ref. [23], but extends the ridge zone to the historical center of Navelli (Figure 9c) that,
300 for this reason, is classified in T3 instead of T2 class. In this regard, the topographic classification map is
301 conservative with respect to a more detailed observation at the site.

302 Finally, the ridge of Assisi, studied by Ref. [22], is presented. The station ASS
303 (http://itaca.mi.ingv.it/ItacaNet_31/#/station/IT/ASS) is located inside the Sacro Convento, near the historical
304 Basilica of San Francesco, at the WWN edge of a 3D relief featuring two 2D appendixes pointing NNE and
305 WWN. The ASS station shows an amplification at 3.5 Hz, polarized at 25°, perpendicularly to the main axis
306 of the ridge. In Ref. [22] the ASS station is indicated in T3 class. The topographic classification map of this

study (Figure 9d) reproduces the morphological features described in Ref. [22], with a T3-T4 class for the WWN edge of the 3D relief.

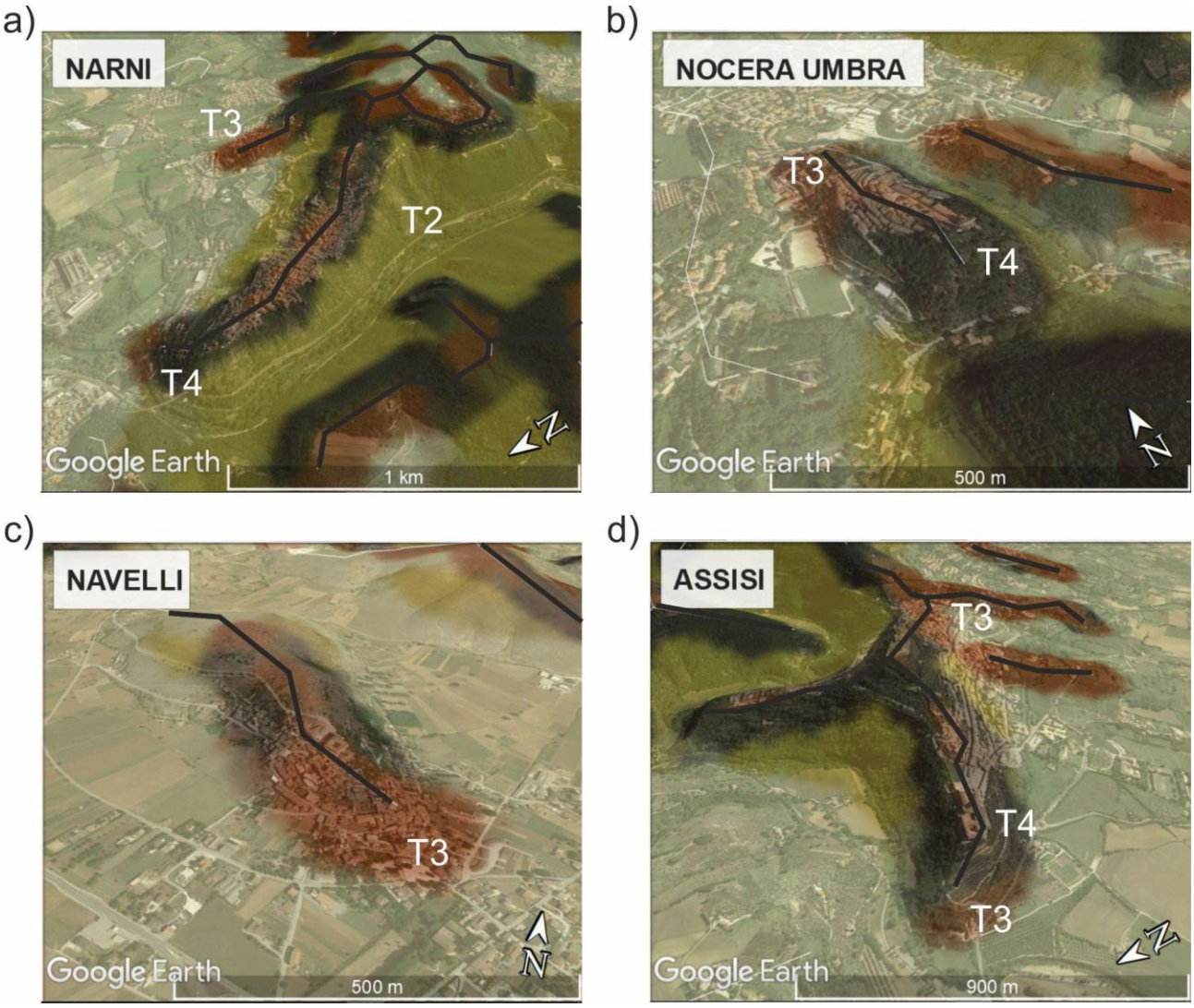

Figure 9. 3D view of the topographic classification map. Narni (a), Nocera Umbra (b), Navelli (c), and Assisi (d). The ridge lines are reported as black solid lines. The legend for color scale is the same as Figure 6.

5. Conclusions

The paper describes a GIS procedure for the topographic classification of a DEM, according to the NTC18 seismic code. The resulting map, with the topographic classification of Italy, is provided in the electronic supplement.

The GIS procedure is easily replicable: it makes use of (i) TinItaly high-resolution DEMs, (ii) the ridges identification with the Topographic Position Index (TPI; [35]), and (iii) slope angle and elevation differences calculated with built-in ESRI ArcGIS functions. The procedure allows to univocally classify the Italian territory and improves previous studies [24], where the classification was only performed in the neighbourhood of a single accelerometric station. Moreover, the results of this study do not need a manual revision, usually performed on Google Earth [48, 49, 38]. In this case, not applying quantitative and systematic morphological analyses based on digital elevation models, the topographic classification is affected by a certain level of subjectivity, related to the point of view, and to the complex geomorphology of the site. The overall check between the topographic map and the case studies reported in this work indicates a satisfactory representation of the morphological features and a correct classification of the sites. In case of mismatch, the proposed classification is generally conservative.

The statistics computed on the topographic classification map show that one third of the Italian territory is characterized by sites with possible topographic amplification (i.e., T2, T3 and T4 classes, Table 1). In particular, following the NTC18 and EC8 seismic codes, 25% of Italian territory is characterized by a topographic amplification factor of 1.2 (T2 and T3 classes), whereas 12% of the country area presents a topographic amplification factor of 1.4 (T4 class). The NTC18 prescribes the applicability of the topographic coefficients in case of "simple" configurations, but the criteria to discriminate between "simple" and "complex" are not specified and, for this reason, the applicability of the coefficients could be debated. Here we propose the application to the entire Italian territory, extending the classification prescribed in seismic codes for "simple" 2D relief configurations to all 3D geomorphological settings. The statistics computed on the 15332 Italian localities in DBMI [32] support the effectiveness of this extrapolation from 2D to 3D, but do not prove the existence of topographic amplification effects. Based on the topographic classification proposed in this study, about 40% of the localities that experienced the highest macroseismic intensities (*Imax* >6) are potentially affected by topographic amplification (T2-T4 classes). The impact of the topographic amplification (Table 1) on the hazard map [30], calculated as PGA for a return period of 475 years and soil category A (NTC18), is shown in Figure 10. Being the topographic amplification period-independent according to NTC18 (Table 1), the effects are the same at all spectral periods.

The map of the topographic classification of Italy can be used for both scientific and application purposes. In this regard, the topographic classification map may be used for the characterization of seismic stations, and may support the identification of sites with systematic topographic effects. The map is also useful for the selection of accelerometric time histories that meet the spectrum-compatibility requirement indicated in the Italian (NTC18) and European (EC8) seismic codes. In the latter case, it allows selecting those stations in T1 class, whose recordings are not affected by topographic amplification. Moreover, the proposed map may guide future investigations of T2, T3 and T4 sites, in particular to study the period-dependent topographic amplifications, as opposed to the constant amplification factors provided in NTC18 and EC8 seismic codes.

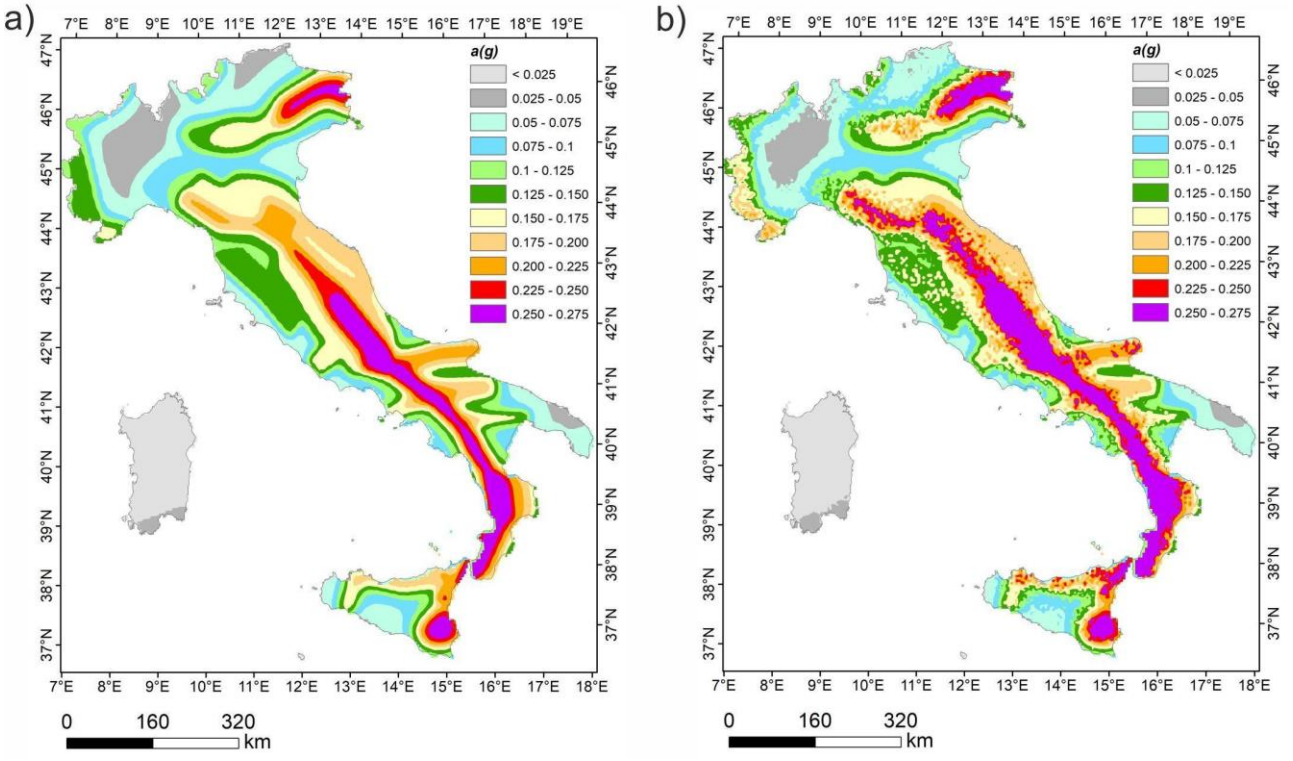

Figure 10: a) probabilistic seismic hazard map for PGA, soil class A and topographic class T1 (return period of 475 years), as in Ref. [30]; b) application of topographic amplification factors according to the classification shown in Figure 6.

Acknowledgment

The study has partially benefited from funding provided by the Italian Presidenza del Consiglio dei Ministri–Dipartimento della Protezione Civile (DPC)—Agreement B2, DPC-INGV. This paper does not necessarily represent DPC official opinions and policies.

CRediT authorship contribution statement

Claudia Mascandola: Conceptualization, Methodology, Software, Writing - original draft, Writing - review & editing, Data curation, Formal analysis. **Lucia Luzi:** Conceptualization, Methodology, Software, Writing - original draft, Writing - review & editing, Data curation, Formal analysis. **Chiara Felicetta:** Writing - original draft, Writing - review & editing, Data curation, Formal analysis. **Francesca Pacor:** Writing - original draft, Writing - review & editing, Data curation, Formal analysis.

References

[1] Boore, D. M. (1972). A note on the effect of simple topography on seismic SH waves, Bull. Seismol. Soc. Am. 62, 275–284.

[2] Bard, P. Y. (1982). Diffracted waves and displacement fields over two dimensional elevated topographies, Geophys. J. Int. 71, 731–760.

[3] Panizza, M. (1991). Geomorphology and seismic risk. Earth-Sci Rev; 31:11–20.

[4] Paolucci, R. (2002). Amplification of earthquake ground motion by steep topographic irregularities. Earthq. Eng. Struct. Dyn.; 31:1831–53.

[5] Griffiths, D.W., and Bollinger, G.A. (1979). The effect of Appalachian Mountain topography on seismic waves. Bull. Seism. Soc. Am.; 69:1081–105.

[6] Kawase, H, and Aki, K. (1990). Topography effect at the critical SV-wave incidence: possible explanation of damage pattern by the Whittier Narrows, California, earthquake of 1 October 1987. Bull. Seism. Soc. Am.; 80:1–22.

388 [7] Marsan, P, Milana, G, Pugliese, A, and Sanò, T. (2000). Local amplification effects recorded by a local
389 strong motion network during the 1997 Umbria-Marche earthquake. In: Proceedings of 12th world conference
390 on earthquake engineering, paper no. 1046. Auckland, New Zealand.

391 [8] Marra, F., Azzara, R., Bellucci, F., Caserta, A., Cultrera, G., Mele, B., Palombo, B., Rovelli, A., and
392 Boschi, E. (2000). Large amplification of ground motion at rock sites within a fault zone in Nocera Umbra
393 (central Italy). J Seismol.;4:543–54.

394 [9] Cara, F., Rovelli, A., Di Giulio, G., Marra, F., Braun, T., Cultrera, G., Azzara R., and Boschi E.(2005).
395 The role of site effects on the intensity anomaly of San Giuliano di Puglia inferred from aftershocks of the
396 Molise, Central Southern Italy, sequence, Bull. Seism. Soc. Am.;95:1457–68.

397 [10] Massa, M., Lovati, S., D'Alema, E., Ferretti, G., and Bakavoli, M. (2010). An experimental approach for
398 estimating seismic amplification effects at the top of a ridge, and the implication for ground-motion
399 predictions: the case of Narni, Central Italy. Bull. Seism. Soc. Am.; 100(6): 286–301.

400 [11] Buech, F., Davies, T.R., and Pettinga, J.R. (2010). The little red hill seismic experimental study:
401 topographic effects on ground motion at a bedrock-dominated mountain Edifice. Bull. Seism. Soc.
402 Am.;100:2219–29.

403 [12] Marzorati, S., Ladina, C., Falcucci, E., Gori, S., Saroli, M., Ameri, G., and Galadini F. (2011). Site effects
404 on the rock: the case of Castelvecchio Subequo (L'Aquila,central Italy). Bull. Earthq. Eng.;9:841–68.

405 [13] Paolucci, R., Faccioli, E., and Maggio, F. (1999). 3D Response analysis of an instrumented hill at
406 Matsuzaki, Japan, by a spectral method. J. Seismol.;3:191–209.

407 [14] Gazetas, G., Kallou, P.V., and Psarropoulos, P.N. (2002). Topography and soil effects in the Ms 5.9
408 Parnitha (Athens) earthquake: the case of Adámes. Nat. Hazards; 27:133–69.

409 [15] Assimaki, D., Gazetas, G., and Kausel, E.. (2005). Effects of local soil conditions and topographic
410 aggravation seismic motion: parametric investigation and recorded field evidence from the 1999 Athens
411 earthquake. Bull. Seism. Soc. Am.; 95:1059–89.

412 [16] Scandella, L, Davì, M, Paolucci, R, and Pessina, V. (2008). Numerical simulation and Gis mapping of
413 seismic amplification due to topographic effects. In: Proceedings of 31st European Seismological Commission
414 (ESC). Crete, Greece.

415 [17] Faccioli, E. (Eds.) (1986). Elementi Per Una Guida Alle Indagini Di Microzonazione sismica – Progetto
416 finalizzato "Geodinamica", Quaderni de "La ricerca scientifica", n.114, CNR, 7, 72–82, (in Italian).

417 [18] Faccioli, E., Vanini, M., Frassine, L. (2002). "Complex" site effects in earthquake ground motion,
418 including topography. In: Proceedings of 12th European Conference on earthquake engineering. Paperno. 844.

419 [19] Galli, P, and Molin, D. (2004). Macroseismic Survey of the 2002 Molise, Italy, Earthquake and Historical
420 Seismicity of San Giuliano di Puglia. Earthq. Spectra; 20(S1):39–52.

421 [20] Tertulliani, A, Arcoraci, L, Berardi, M, Bernardini, F, Camassi, R, Castellano, C, Del Mese, S., Ercolani,
422 E., Graziani, L., Leschiutta, I., Rossi A., and Vecchi M. (2011). An application of EMS98 in a medium-sized
423 city: the case of L'Aquila (Central Italy) after the April 6, 2009 Mw 6.3 earthquake. Bull. Earthq. Eng; 9:67–
424 80.

425 [21] Gizzi, F.T., Potenza, M.R., and Zotta, C. (2012). 3 November 1980 Irpinia-Basilicata earthquake
426 (Southern Italy): towards a full knowledge of the seismic effects. Bull. Earth. Eng; 10:1109–31.

427 [22] Cauzzi, C., Fäh, D., Pessina, V., Faccioli, E., and Smerzini, C. (2012). Topographic amplification from
428 recorded earthquake data and numerical simulations. In 15th World Conference on Earthquake Engineering.

429 [23] Gallipoli, M. R., Bianca, M., Mucciarelli, M., Parolai, S., and Picozzi, M. (2013). Topographic versus
430 stratigraphic amplification: mismatch between code provisions and observations during the L'Aquila (Italy,
431 2009) sequence. Bull. of Earth. Eng., 11(5), 1325-1336.

[24] Pessina, V., and Fiorini, E. (2014). A GIS procedure for fast topographic characterization of seismic recording stations. Soil Dynamics and Earthquake Engineering, 63, 248-258.

[25] NTC (2018). Ministero delle Infrastrutture e dei Trasporti. Aggiornamento delle Norme Tecniche per le Costruzioni. Part 3.2.2: Categorie di sottosuolo e condizioni topografiche, Gazzetta Ufficiale n. 42 del 20 febbraio 2018 (in Italian).

[26] CEN (Comite Europe en de Normalisation), 2004. Eurocode 8. Design Provisions for Earthquake Resistance of Structures—Part 5: Foundations, Retaining Structures and Geotechnical Aspects. ENV 1998-5, CEN European Committee for Standardisation, Brussels, 1994.

[27] NTC (2008). Ministero delle Infrastrutture e dei Trasporti. Nuove Norme Tecniche per le Costruzioni. Part 3: Categorie di sottosuolo e condizioni topografiche, Gazzetta Ufficiale, no. 29, del 4 febbraio 2008 (in Italian).

[28] Luzi, L., Hailemikael, S., Bindi, D., Pacor, F., Mele, F., and Sabetta, F. (2008). ITACA (ITalian ACcelerometric Archive): A Web Portal for the Dissemination of Italian Strong-motion Data, Seismological Research Letters, 79(5), 716–722.

[29] Pacor, F., Paolucci, R., Luzi, L., Sabetta, F., Spinelli, A., Gorini, A., Nicoletti, M., Marcucci, S., Filippi, L., and Dolce M. (2011), Overview of the Italian strong motion database ITACA 1.0, Bull. Earth. Eng, 9(6), 1723–1739.

[30] MPS Working Group (2004). Redazione della mappa di pericolosità sismica prevista dall'Ordinanza PCM del 20 marzo 2003, Rapporto Conclusivo per il Dipartimento della Protezione Civile (in Italian).

[31] Stucchi, M., C. Meletti, V. Montaldo, H. Crowley, G. M. Calvi, and E. Boschi (2011). Seismic hazard assessment (2003–2009) for the Italian building code, Bull. Seismol. Soc. Am. 101, no. 4, 1885–1911.

[32] Locati, M., Camassi, R., Rovida, A., Ercolani, E., Bernardini, F., Castelli, V., Caracciolo, C.H., Tertulliani, A., Rossi, A., Azzaro, R., D'Amico, S., Conte, S., Rocchetti, E., Antonucci, A. (2019). Database

455 Macrosismico Italiano (DBMI15), versione 2.0. Istituto Nazionale di Geofisica e Vulcanologia (INGV).
456 https://doi.org/10.13127/DBMI/DBMI15.2

457 [33] D'Amico, M., Felicetta, C., Russo, E., Sgobba, S., Lanzano, G., Pacor, F., and Luzi, L. (2020). Italian
458 Accelerometric Archive v 3.1 - Istituto Nazionale di Geofisica e Vulcanologia, Dipartimento della Protezione
459 Civile Nazionale. doi: 10.13127/itaca.3.1

460 [34] Tarquini, S., Isola, I., Favalli, M., Mazzarini, F. ,Bisson, M., Pareschi, M.T., and Boschi, E. (2007).
461 TINITALY/01: a new triangular irregular network of Italy. Annals of Geophysics 50,407–425.

462 [35] Weiss, A. (2001). Topographic position and landform analysis. Poster presentation, ESRI Users
463 Conference, San Diego, CA.

464 [36] Burrough, P. A., and McDonell, R. A., (1998). Principles of Geographical Information Systems (Oxford
465 University Press, New York), 190 pp.

466 [37] Jenness, J., Brost, B., and Beier, P. (2013). Land facet corridor designer. USDA forest service rocky
467 mountain research station.

468 [38] Mascandola, C., Massa, M., Lovati, S., and Augliera, P. (2018). The site characterization scheme of the
469 INGV strong motion database (ISMD): Overview and site classification. Seism. Res. Lett., 89(1), 86-98.

470 [39] Zhan, C. (1993). A Hybrid Line Thinning Approach. Proceedings Auto-Carto 11, Minneapolis, pp. 396-
471 405.

472 [40] OPCM n. 3519 (2006): criteri generali per l'individuazione delle zone sismiche e per la formazione e
473 l'aggiornamento degli elenchi delle stesse zone; Gazzetta Ufficiale n. 108 dell'11 maggio 2006 (in Italian).

474 [41] ISTAT, 2011. 154° Censimento della Popolazione e delle Abitazioni. http://www.istat.it/it/censimento-
475 popolazione/censimento-popolazione-2011.

476 [42] Sieberg, A. (1930). The earthquake geology (Geologie der Erdbeben). Handbuch der Geophysik
477 2(4):550–555 (in German).

[43] Caserta, A., Bellucci, F., Cultrera, G., Donati, S., Marra, F., Mele, G., Palombo, B. and Rovelli, A. (2000). Study of site effects in the area of Nocera Umbra (Central Italy) during the 1997 Umbria-Marche seismic sequence, J. Seismol., 4, 555–565.

[44] Donati, S., Marra, F. and Rovelli, A. (2001). Damage and ground shaking in the town of Nocera Umbra during Umbria-Marche, central Italy, earthquakes: the special effect of a fault zone, Bull. seism. Soc. Am., 91, 511–519.

[45] Pischiutta, M., Cultrera, G., Caserta, A., Luzi, L., and Rovelli, A. (2010). Topographic effects on the hill of Nocera Umbra, central Italy. Geophysical Journal International, 182(2), 977-987.

[46] Lovati, S., Bakavoli, M. K. H., Massa, M., Ferretti, G., Pacor, F., Paolucci, R., Haghshenas E., and Kamalian, M. (2011). Estimation of topographical effects at Narni ridge (Central Italy): comparisons between experimental results and numerical modelling. Bull. of Earth. Eng., 9(6), 1987-2005.

[47] Pischiutta, M., Cianfarra, P., Salvini, F., Cara, F., and Vannoli, P. (2018). A systematic analysis of directional site effects at stations of the Italian seismic network to test the role of local topography. Geophysical Journal International, 214(1), 635-650.

[48] Pessina, V. (2010). Appendix E. EC8 subsoil and topographic classification of ITACA stations Deliverable D10, Project S4 The Italian strong motion database. http://esse4.mi.ingv.it/files/images/stories/d10_appendix%20e.pdf

[49] Di Capua, G., Lanzo, G., Pessina, V., Peppoloni, S., and Scasserra, G. (2011). The recording stations of the Italian strong motion network: Geological information and site classification. Bulletin of Earthquake Engineering, 9(6), 1779-1796.

Declaration of interests

☒ The authors declare that they have no known competing financial interests or personal relationships that could have appeared to influence the work reported in this paper.

☐The authors declare the following financial interests/personal relationships which may be considered as potential competing interests:

CRediT authorship contribution statement

Claudia Mascandola: Conceptualization, Methodology, Software, Writing - original draft, Writing - review & editing, Data curation, Formal analysis. **Lucia Luzi:** Conceptualization, Methodology, Software, Writing - original draft, Writing - review & editing, Data curation, Formal analysis. **Chiara Felicetta:** Writing - original draft, Writing - review & editing, Data curation, Formal analysis. **Francesca Pacor:** Writing - original draft, Writing - review & editing, Data curation, Formal analysis.